CHARACTERIZATION OF THE ROLE OF NUCLEAR LOCALIZED TYPE IV SECRETION SUBSTRATES IN *COXIELLA BURNETII* PATHOGENESIS

A Dissertation

by

SARA JEAN TALMAGE

Submitted to the Office of Graduate and Professional Studies of
Texas A&M University
in partial fulfillment of the requirements for the degree of

DOCTOR OF PHILOSOPHY

Chair of Committee,	James Samuel
Committee Members,	Paul de Figueiredo
	Jon Skare
	Joesph Sorg
Head of Department,	Warren Zimmer

August 2019

Major Subject: Medical Sciences

ABSTRACT

The nucleus is the brain of the cell and is the site of regulation of processes such as DNA replication, transcription and cell cycle. Given its importance in cell function, several known bacterial proteins have been shown to modulate nuclear processes to co-opt the host cell for the benefit of the bacteria. Such proteins, termed nucleomodulins, can modulate either nuclear DNA or proteins through a variety of mechanisms. *Coxiella burnetii* is a Gram negative, obligate intracellular pathogen and the etiological agent of the zoonotic disease known as Q fever. The goal of this project is to determine if *C. burnetii* employs any of its type IVB secretion system (T4SS) substrates to act as nucleomodulins. In a large-scale screen of T4BSS substrates, we showed six substrates that exhibited nuclear localization when expressed ectopically in HeLa cells. Bioinformatic analysis revealed that two of these potential Nucleomodulins, CBU0388 and CBU0794, contained potential nuclear localization signals (NLS). We tested the functionality of these regions by making specific amino acid deletions and comparing the impact on their nuclear localization patterns. To predict functionality of these substrates, we conducted an Epistasis Miniarray profile (EMAP) screen in *S. cerevisiae* which provided a global quantitative genetic profile of host interactions. Our results support our hypothesis these two previously uncharacterized *C. burnetii* substrates act uniquely as nucleomodulins in the host cell.

DEDICATION

To Edward and Eleanor

ACKNOWLEDGEMENTS

I would like to thank my dissertation committee, Drs. James Samuel, Paul de Figueiredo, Jon Skare, and Joseph Sorg for their guidance during my time in graduate school.

I also want to extend my gratitude to my friends and colleagues and the department faculty and staff in the Department of Microbial Pathogenesis and Immunology for all their continued support. A special thanks goes to Elizabeth Case and Erin van Schaik, who served as invaluable resources to me during my graduate studies.

Finally, thanks to my family, especially to my husband for constant encouragement and patience.

CONTRIBUTORS AND FUNDING SOURCES

Contributors

This work was supported by a dissertation committee consisting of Professor James Samuel, Jon Skare, and Paul de Figueiredo of the Department of Microbial Pathogenesis and Immunology and Professor Joseph Sorg of the Department of Biology.

The EMAP data was done in collaboration with Dr. Kristin Patrick, Dr. Robert Watson and the Krogen laboratory and was published in *Cell Systems* (2018).

The RNA-seq and BMDM experiments were done in part by Elizabeth Case in the Samuel laboratory. The SCID mouse experiments were designed and assisted by Erin van Schaik.

Larry Dangot from the Protein Chemistry lab at Texas A&M University did the mass spectrometry analysis. Jane Miller assisted in running flow cytometry. From the Texas A&M Institute for Genome Sciences and Society, Andrew Hillhouse ran the RNA-seq and whole genome sequencing and Kranti Kongati did the bioinformatic analysis.

The student completed all other work for the dissertation individually.

Funding Sources

This project was supported by the Defense Threat Reduction Agency (HDTRA1-13-1-0003) and NIH/NIAID (5R01AI090142-01A1). Its contents are solely the responsibility of the authors and do not necessarily represent the official views of DTRA, or NIH

NOMENCLATURE

ACCM-2	Acidified Citrate Cysteine Medium
BSL2	Biosafety Level 2
CCV	Coxiella-containing vacuole
Dot/Icm	Defect in organelle trafficking/intracellular multiplication
DNA	Deoxyribonucleic acid
EHEC	Enterohemorragic *Esherichia coli*
EPEC	Enteropathogenic *Esherichia coli*
IPZ	Importazole
ISGs	Interferon-stimulated genes
LepB	Leptomycyin B
LPS	Lipopolysaccharide
NES	Nuclear export signal
NLRs	Nod-like receptors
NLS	Nuclear localization signal
PS	Phosphatidylserine
RNA	Ribonucleic acid

TABLE OF CONTENTS

Page

LIST OF FIGURES

Page

LIST OF TABLES

Page

CHAPTER I

INTRODUCTION AND LITERATURE REVIEW

Coxiella burnetii Disease and Intracellular lifecycle

C. burnetii is an obligate intracellular pathogen and the etiological agent of Q fever, a zoonotic disease spread through aerosoliziation of contaminated animal products [1]. This disease is readily transmitted with a low infectious dose by aerosol and has potential to be a bioterrorist weapon, so thus has been classified as a category B select agent [2]. After transmission of aerosolized particles, the organism displays specificity for infecting primary alveolar macrophages.

The natural hosts for *C. burnetii* include cows, sheep, and goats, with human infection being a result of exposure to contaminated animal products. This makes *C. burnetii* infections endemic to farming communities. The most recent notable outbreak occurred between 2007 and 2009 in the Netherlands and resulted in 3,523 cases of disease [3]. The resulting disease, termed Q fever, from its original name of Query fever was defined when the causative agent was discovered in the 1930s [4]. Symptoms of Q fever include a flu-like illness with high cyclic fever, although infection often can be asymptomatic. The treatment of choice of *C. burnetii* infection is doxycycline, which has been very effective against acute Q fever. In rare cases, Q fever can become chronic and have localized complications such as endocarditis, hepatitis, or myocarditis [5].

Q-Vax, a whole-cell vaccine available in Australia has been shown to be effective at preventing *C. burnetii* infection. Unfortunately, this vaccine elicits an

adverse response in individuals with prior exposure to the bacterium [6]. Current research by our lab, and others, is ongoing to identify a vaccine that is protective and does not have these adverse responses.

The virulent Phase I organisms possesses smooth lipopolysaccharide (LPS) that, upon serial passage, undergoes a phase variation to an avirulent Phase II, with rough LPS [7]. This phase variation is due to a truncated O antigen on Phase II which lacks terminal sugars [8]. Since this is the only difference between virulent Phase I and avirulent Phase II, the full-length LPS is thought to be essential for virulence [9]. Phase II is approved to be handled in Biosafety Level 2 conditions (BSL2), while Phase I is restricted in a Biosafety Level 3 and Select Agent registered laboratory. Phase I and Phase II *C. burnetii* behave similarly during infection, so Phase II is commonly used for research [10]. Phase I and Phase II act similarly in replication kinetics and have an indistinguishable lifecycle in a *Coxiella*-containing vacuole (CCV), so most cellular mechanisms are studied in Phase II [10].

C. burnetii survives in the environment due to its ability to switch between two morphological forms that can be sectored into developmental stages. In the first stage, the small cell variant (SCV) is metabolically inactive and resistant to environmental changes. The SCV is also the infectious form, which upon entry into the host cells switches to the large cell variant (LCV) [11]. The LCV is the larger replicative form, which is only found inside cells. Because of this environmental stability, transmission of *C. burnetii* has also been shown to be transmitted through human or blood contact [12].

Upon aerosolization, *C. burnetii* enters the cell through a passive process that requires actin-dependent phagocytosis [13]. Virulent Phase I *C. burnetii* binds to phagocytes by using $\alpha_V\beta_3$ as its main endocytosis receptor, which results in RAC1-dependent phagocytosis; the *C. burnetii* ligand for binding the receptor is still unknown [14]. Despite its trophism for alveolar macrophages, *C. burnetii* is capable of infecting many cell types. Although the receptor of non-phagocytic cells is unknown, entry requires cytoskeletal rearrangement [15]. Following uptake by the cell, *C. burnetii* utilizes the endocytic pathway to set up its replicative niche , the CCV [16].

The CCV is a unique replicative niche compared to most other intracellular organisms. *C. burnetii* makes its home in what is typically considered to be a terminal phagolysosome which contains typical markers that stain this organelle such as Lamp1 and Rab7 [17] . The full list of proteins associated with the CCV is not known, unfortunately, so there is a lack of understanding of all the requirements for *C. burnetii* growth in its replicative niche. Fusion of the autophagosome with lysosomes causes acidification of vacuole contents to a pH of about 4.5, too acidic for most bacteria to survive. This acid adaptation is a requirement for *C. burnetii* replication to occur inside the vacuole [18]. This vacuole fusion and acidification is not unique to only *C. burnetii*. Interestingly, *C. burnetii* can share a vacuole with *Mycobacterium tuberculosis* and *Mycobacterium avium* [19], *Trypanosoma cruzi* [20, 21], *Leishmania amazonensis* [22], and *Salmonella enterica* [23].

Secretion systems

The genome of *C. burnetii* encodes a Sec-dependent secretion system, as well as a type Ia, type II, a type IV pilus and a type IV secretion system [24]. The *C. burnetii* type IV secretion system is homologous to the Dot/Icm system (*d*efect in *o*rganelle *t*rafficking/*i*ntrac*e*llular *m*ultiplication) of *Legionella pneumophila*, (encoding 23 of the 26 genes from *L. pneumophila*) [25]. The functional homology was further supported n by the ability of *L. pneumophila* to cross-complement mutants of *C. burnetii* in structural components of the Dot/Icm system [26, 27]. *C. burnetii* uses the Dot/Icm system to secrete and deliver a number of effector proteins into the host cytosol for modulation of the host cell. The Dot/Icm secretion system in *C. burnetii* is required for important cellular functions including intracellular replication and vacuole formation, as both of these processes are defective in any Dot/Icm mutant [28]. Because of the similarity between their Dot/Icm secretion systems, *L. pneumophila* has been used as a surrogate host in multiple screens to test predicted candidates for secretion [29-31]. To date, secretion studies as well as bioinformatic screens have identified over 100 Dot/Icm substrates [30-33] encoded by the Nine Mile strain.

Animal Models

Animal models of Q fever have been elusive since Phase II *C. burnetii* has limited virulence in an immunocompetent host animal. To circumvent this problem, our lab developed a mouse model using SCID mice, which lack functional B and T cells to provide a model of human infections of immunocompromised hosts with this strain [34].

This mouse model shows bacterial replication, massive splenomegaly and dissemination to multiple tissues including the spleen, lungs and heart. The SCID mouse model has provided a unique tool to study *Himar1* transposon mutants and their potential contribution to virulence.

In addition to the SCID mouse model, a moth model using *Gallaria mellonella* has also recently been developed [35]. This model provides a tool for studying potential virulence determinants in *C. burnetii.* This model is economical and especially good for high-throughput analyses. The major limitation to this model is that *Gallaria* cannot fully mimic the mammalian host response because it lacks specific components, including NOD-like receptors (NLRs) [36].

Genetic Tools

Genetic manipulation in *C. burnetii* is a relatively recent advancement. The genome was sequenced in 2003, a little over a decade ago [24]. Since then, experimental advances have enabled limited genetic manipulation of the bacteria. A successful transformation of an exogenous plasmid into *C. burnetii* was first reported nearly fifteen years ago [37]. Despite this, it wasn't until more recent years that introduction of a plasmid genetic system could allow us to create a targeted gene mutation [38].

An axenic (cell-free) media system, Acidified Citrate Cysteine Medium (ACCM-2) permits growth of *C. burnetii* outside of tissue culture cells [39, 40]. This medium uses an acidic pH and microaerophillic conditions to replicate the naturally intracellular environment for *C. burnetii* growth. This media can also be used to make agar plates, so individual clones of *C. burnetii* on plates can be isolated. Since the initial ACCM-2

formula, improvements have been made to allow arginine selection, based on *C. burnetii* auxotrophy for the amino acid Arginine [41]. Development of ACCM-2 has now allowed gene inactivation in *C. burnetii* to be possible. Our lab and others have developed a *mariner*-based *Himar1* transposon system to generate a random library of mutants, a technique we are continuing to optimize for creation of an expanding library.

Current state of effector research

Despite recent genetic advances in *C. burnetii,* there still remains a huge gap in understanding of the functions of most T4SS effectors. To date, only a handful of T4SS effectors have been characterized and a number of screens have been done to identify effectors and their potential function [30, 31, 42]. These screens identified potential effectors based on homology to Dot/Icm substrates of *L. pneumophila*, PmrA regulation sites, presence of eukaryotic-like motifs and secretion in a CyA or BlaM assay. Collectively these screens identified greater than 100 Dot/Icm effectors in *C. burnetii,* but few have been fully characterized.

Two of the best-characterized *C. burnetii* effectors are Cig2 (also called CvpB) and Cig57. Both of these effectors were identified through a screen of transposon mutants looking to identify mutants that were required for CCV biogenesis [43]. Interestingly, the mutants identified in this screen displayed unique phenotypes in regards to vacuole formation. Mutants in Cig57 showed decreased replication despite the ability to form a spacious vacuole. Also unique to previously identified phenotypes, mutants in Cig2 displayed a multi-vacuolar phenotype suggesting that they lack the

ability to fuse their CCVs, resulting in multiple small vacuoles.

Since their initial identification, Cig57 has been shown to interact directly with the clathrin-associated protein FCHO2 [44]. This interaction was dependent on an endocytic-sorting motif found in Cig57. Further, knockdown experiments showed that clathrin recruitment to the CCV by Cig57 was important for promotion of full vacuole expansion.

Two different studies followed up on the multi-vacuolar phenotype of Cig2. The first study showed that Cig2 binds to two host lipids PI[45]P and phosphatidylserine (PS) on the CCV to co-opt the autophagy machinery and promote homotypic fusion [46]. This same study also used the *G. mellonella* model to show the *in vivo* requirement of Cig2 for pathogenesis of *C. burnetii.* The second study by a different research group highlighted the role of Cig2 in promoting host autophagy and recruitment of autophagy receptors onto the CCV [47]. These studies of both Cig57 and Cig2 are notable in the field of *C. burnetii* for being two of the few instances where a molecular mechanism was attributed to the role of a secreted effector.

Nuclear Effectors

Recently, the importance of a new class of secreted effectors that impact nuclear processes, termed nucleomodulins, have emerged. Nucleomodulins have been shown to be intimately involved in controlling the host cell gene expression, RNA splicing, DNA replication and repair, and chromatin remodeling for the benefit of the bacteria [48]. A

notable example of a well-characterized nucleomodulin is LntA from *Listeria monocytogenes.* This effector has been shown to control innate immune responses to infection by binding to the chromatin-silencing complex BAHD1, which prevents it from binding to promoter regions of interferon-stimulated genes (ISGs) [49]. This allows an increase in chromatin unwinding and acetylation of histone H3 and an upregulation of ISG expression, a response that has been shown to be in favor of the bacteria [50, 51].

A specific class of nucleomodulins, termed cyclomodulins, has the ability to affect host cell cycle and have also shown to be important for the bacteria survival in a host cell [52, 53]. The most well-characterized of this class is the effector Cif, cycle-inhibiting factor. This effector is secreted by both Enteropathogenic *Esherichia coli* (EPEC) and Enterohemolytic *E. coli* (EHEC), causative agents of bacterial diarrhea. This effector blocks cellular mitosis by preventing Cdk1 action, arresting cells in the G_2/M stage of cell cycle [54]. Both LntA and Cif are only two examples of bacterial secreted effectors that modulate the host nucleus, but they highlight the importance of this novel class.

There are six effectors in *C. burnetii* that have been published to have nuclear localization when a tagged version is transiently transfected into host epithelial cells [31]. Those effector proteins are: CBU0129, CBU0388, CBU0393, CBU0794, CBU1314 and CBU1524. Although not identified in that initial screen, AnkG was shown to exhibit nuclear trafficking in its role in preventing apoptosis [55]. Prior work described a potential role CBU1314 may play in modulating transcription [56], although

these results have not been fully confirmed. Another study has elucidated a role for CBU1524, named CaeA (*Coxiella* anti-apoptotic effector A), in preventing apoptosis when transiently expressed in epithelial cells [57]. A subsequent study demonstrated that CaeA contains an EK (glutamic acid/lysine) motif that is required for inhibiting apoptosis [58]. In addition, the authors found that expression of CaeA resulted in the upregulation of Survivin, a protein inhibitor of caspases that prevents apoptosis. Although no mutation has been reported for CaeA, AnkG or CBU1314 to test their role during infection, there is potential that they represent crucial effector proteins. Arguably, the presence of seven unique T4SS effector proteins in the nucleus supports the importance for host nuclear manipulation by *C. burnetii*.

CHAPTER II

THE COXIELLA BURNETII TYPE IV SECRETION EFFECTOR CBU0794 INTERACTS WITH HOST NUCLEAR PROTEIN TBL1XR1

Synopsis

Coxiella burnetii is an obligate intracellular pathogen and the causative agent of Q fever. One of the main virulence factors to promote survival and replication inside host cells is the type 4b (dot/icm) secretion system. Using ectopic localization of transfected HeLa cells, we previously identified 6 T4SS effectors that localize to the nucleus. To investigate the functionality of one of these, CBU0794, we deleted the bioinformatically-predicted nuclear localization signals (NLSs). This revealed a single NLS required for nuclear translocation. Furthermore, protein interaction studies revealed a novel interacting partner, TBL1XR1, a key transcriptional regulator. Consequences of this interaction are still yet to be determined, but they could provide insight to important transcriptional pathways for *C. burnetii*.

Introduction

C. burnetii is a Gram negative intracellular bacterium and the causative agent of the zoonotic disease, Q fever. The organism is spread through transmission of contaminated animal products, commonly by aerosols. Although the organism primarily targets alveolar macrophages, it can spread and infect other tissue types. Aerosol transmission, high infectivity, and stability in the environment resulted in its classification as a category B select agent and potential bioterrorist threat.

Once inside the host cell, *C. burnetii* employs its type IVB secretion system (T4SS) that secrete effector proteins to help establish its intracellular niche. While over 100 potential secreted proteins have been identified [45], most of them lack much data as to their function. While new genetic tools have allowed some genetic mutant screens, most functional data we have for these effectors come through ectopic expression. This allows us to specifically query the direct effects of the protein itself without relying on complicated infection dynamics including host response and nutritional requirements. While this has an array of caveats, ectopic data has allowed more functional data to be understood [56, 59].

CBU0794 (Cig20) was initially identified as a T4BSS effector because the promoter region has a predicted PmrA binding site, suggesting this gene is co-regulated with *icm* genes [42]. Our lab previously demonstrated that CBU0794 localizes to the nucleus when transiently transfected into HeLa cells [31]. In this study, we further investigated the nuclear interactions affected by CBU0794. Here we show that

CBU0794 trafficking to the nucleus is dependent on a single canonical nuclear localization signal, where it then interacts with TBL1XR1, which has multiple roles in transcriptional regulation. We also show the yeast genetic profile interactions using an epistasis mini-array profile (EMAP) screening assay.

Materials and Methods

Cell Lines and Strains. Strains used in this study are listed in Table 3.2. *C. burnetii* Nine Mile phase II (strain RSA439, clone 4). HeLa cells were used for microscopy experiments and HEK293T cells were used for protein pulldown and RNA-seq.

Cloning and plasmids. Bioinformatic predictions of nuclear localization signals were generated using cNLSmapper (http//nls-mapper.iab.keio.ac.jp/) and/or NLStradamus (http://www.moseslab.csb.utoronto.ca/NLStradamus/). Nuclear export signals were identified through the online bioinformatics tool NetNES 1.1 Server (http://www.cbs.dtu.dk/services/NetNES/). Coiled-coil prediction was found using SMART (http://smart.embl-heidelberg.de/help/smart_glossary.shtml) [60]. Genes were amplified by PCR using Accuprime *Pfx*. PCR products were inserted into the specific plasmid using the In-Fusion system (BD Clontech).

Cell transfection and Inhibitor Treatment. For ectopic expression in mammalian cells, HeLa cells (ATCC CCL-2) were seeded at 60% confluence in a 24-well plate. The following day, cells were transiently transfected with Lipofectamine 3000 according to manufacturer's protocol. For treatment with Importazole (Sigma-Aldrich), cells were transfected for eleven hours following addition of 10μM for 1 hour before fixing.

Fluorescence Microscopy. At indicated timepoints, cells were fixed with 4% paraformaldehyde in PBS at room temperature for 10-15 minutes. After fixation, cells were rinsed in PBS and quenched with 50mM ammonium acetate at room temperature for 10 minutes. Coverslips were then incubated in blocking buffer (0.02% Saponin in PBS with 10% horse serum) for 30 minutes in the dark. After blocking, the coverslips were incubated in the dark with primary antibody diluted in blocking buffer for 1hr at room temperature in the dark. Coverslips were then rinsed and incubated for another hour with each indicated secondary antibody as needed. To visualize the nucleus, coverslips were stained with 10 mg/mL of Hoescht in water for 10 minutes before a final wash with water. Coverslips were mounted on slides with Mowiol and imaged with a Nikon A1 confocal microscope. The Nikon elements software was used for image analysis and quantification.

Protein pulldown. 293T cells were transfected for 24 hours before washing with PBS + 0.5M EDTA. Washed cells were lysed in cell lysis buffer (cell signaling) with protease inhibitor cocktail (cell signaling) and PMSF. GFP resin bead were washed with wash buffer containing 1M Tris pH 7.4, 5M NaCl, 0.5M EDTA, and 20% NP40. Lysates were incubated with anti-GFP beads from the GFP-trap kit (Chromtek) according to the manufacture's protocol. Elution was boiled in 2X Sample buffer (Bio-Rad) and supernatant was used. Protein bands were visualized by Silver Stain (Fisher Scientific) before being analyzed by mass spectrometry.

Western Blotting. Cell lysates were run on a SDS-page gel at 100V for 60 minutes before wet transfer to a PVDF membrane. Immunoblots were performed using rabbit

anti-TBL1XR1 (abcam or Thermo Fisher), or rabbit anti-SMRT (abcam), or rabbit anti-NCoR (abcam) at a 1:5000 dilution. Mouse anti-actin (abcam) was used at a 1:5000 dilution for a loading control. Goat monoclonal anti-mouse (LICOR) and donkey monoclonal anti-rabbit (LICOR) were used at dilutions of 1:10000.

Quanitative RT-PCR. Cells were harvested with TRIzol (Thermo Fisher) and RNA was isolated using a spin column (Machery-Nagel). We made cDNA with the High-capacity Reverse-transcriptase kit (ABI) before using Fast SYBER green (Thermo Fisher) master mix to analyze for specific transcripts in each sample.

RNA-seq. 293T cells were transfected with each construct using PolyJet according to the manufacturers protocol. After 24 hours, cells were treated with Trizol (Invitrogen). Library preparation and sequencing was done at the Texas A&M Institute for Genome Sciences and Society (TIGSS) in College Station, TX. Analysis used either Mock transfected or GFP as a baseline for identifying differentially expressed transcripts with either a 2-fold or 3-fold log increase or decrease.

Yeast toxicity and EMAP analysis. The toxicity assay and EMAP analysis was performed as previously described [61]. Results were determined from at least three independent experiments.

Statistical Analyses. Statistical analysis was performed with Prism (GraphPad Software, Inc.) using an unpaired, Student's t-test. *$P<0.05$, **$P<0.01$.

Table 2.1. Bacterial strains and plasmids used in this study

Strain or Plasmid	Description	Source
Strains		
E. coli DH5α	F– Φ80*lac*ZΔM15 Δ(*lac*ZYA-*arg*F) U169 *rec*A1 *end*A1 *hsd*R17 (rK–, mK+) *pho*A *sup*E44 λ– *thi*-1 *gyr*A96 *rel*A1	Stratagene
E. coli Stellar Cells	F–, endA1, supE44, thi-1, recA1, relA1 gyrA96, phoA, Φ80□ lacZΔ M15, Δ(lacZYA - argF) U169, Δ(mrr - hsdRMS - mcrBC) ΔmcrA, λ–	Clontech
C. burnetii Nine Mile (RSA439)	Phase II, Clone 4	
RSA439 MK	DotA::Tn, Cm^r	
Plasmids		
pEGFP-C1	C-terminal fusion to EGFP, Kan^r	Clontech
pEGFP-C1 0794	CBU0794 cloned into pEGFP-C1	[31]
pEGFP-C1 0794ΔNLS1	CBU0794Δ NES cloned into pEGFP-C1	this study
pEGFP-C1 0794ΔNLS2	CBU0794Δ NLS cloned into pEGFP-C1	this study
pEGFP-C1 0794ΔCC	CBU0794Δ CC cloned into pEGFP-C1	this study

Table 2.2. Oligonucleotides used in this study

Oligonucleotide	Oligonucleotide Sequence (5'-3')	Application
in794dNLS1 Sal F1	GAATTCTGCAGTCGACATGAAAATTATT AAATTAGTGGAA	Infusion deletion of the NLS1
in794dNLS1 Sal R1	TATAGACGAGATAGAGTCTTGAGCTGCTCTATAC	
in794dNLS1 Sal F2	TCTATCTCGTCTATAGATGAA	
in794dNLS1 Sal R2	CCGCGGTACCGTCGACTTATCTAAATCTGGCTTTTTGC	
in794dNLS2 Sal F1	GAATTCTGCAGTCGACATGAAAATTA TTAAATTAGTGGAA	Infusion deletion of NLS2
in794dNLS2 Sal R1	TTCATCCTTATCTCTCGCTTGTCGTGTTCATCAC	
in794dNLS2 Sal F2	AGAGATAAGGATGAACTCCA	
in794dNLS2 Sal R2	CCGCGGTACCGTCGACTTATCTAAATCTGGCTTTTTGC	
in794dCC Sal F1	GAATTCTGCAGTCGACATGAAAATTATTAAA TTAGTGGAA	Infusion deletion of CC domain
in794dCC Sal R1	TCTTTTTCTAATTCGAAAAAGAGATGCAAAACTTTAAA	
in794dCC Sal F2	CGAATTAGAAAAAGAAAATTATTA	
in794dCC Sal R2	CCGCGGTACCGTCGACTTATCTAAATCTGGCTTTTTGC	
794in Tn7HA F	ATTTACGCGTGAATTCATGAAAATTAT TAAATTAGTGGAA	Infusion with EcoRI site into pTN7 TetRA 3xHA

Table 2.2. Oligonucleotides used in this study continued.

Oligonucleotide	Oligonucleotide Sequence (5'-3')	Application
794in Tn7HA R	GCTTCTCGAGGAATTCTTATCTAAATCTGGCTTTTTGC	
hGAPDH F	GGAGCGAGATCCCTCCAAAAT	qPCR
hGAPDH R	GGCTGTTGTCATACTTCTCATGG	qPCR
hNCOR2 F	CACGAGGTGTCAGAGATCATCG	qPCR
hNCOR2 R	GCCATAAGCCCGTTCATGTTG	qPCR
mNCOR2 F	GATGACCCCATGAAGGTCTACA	qPCR
mNCOR2 R	GGCCAAAGTTCTTAGGGTGCT	qPCR
mIL6 F	CCAAGAGGTGAGTGCTTCCC	qPCR
mIL6 R	CTGTTGTTCAGACTCTCTCCCT	qPCR
mCXCL2 F	CCAACCACCAGGCTACAGG	qPCR
mCXCL2 R	GCGTCACACTCAAGCTCTG	qPCR
hTBL1XR1 F	CACCCGCTGCATTGATTTCTA	qPCR
hTBL1XR1 R	TACGGCATCTATCAGGGACAG	qPCR
mTBL1XR1 F	TGCAAGCACACCTGACAAGTT	qPCR
mTBL1XR1 R	CTCCTGTGAATCCAGCTTCTG	qPCR
hNCOR1 F	ACACCGCAGTATTGTCCAAAT	qPCR
hNCOR1 R	CACCTGGTTTGTCTTGATGTTCT	qPCR
mNCOR1 F	ACAGAGCAAAGTCGTTATCCTTC	qPCR

Table 2.2. Oligonucleotides used in this study continued.

Oligonucleotide	Oligonucleotide Sequence (5'-3')	Application
mNCOR1 R	GAGCGGTAGTCAGGAACTGC	qPCR

Results

CBU0794 is expressed during *C. burnetii* infection. In order to assess the expression level of CBU0794, we designed gene specific primers and quanitifed expression both during ACCM-2 growth and different timepoints during infection. As shown in Figure 2.1, expression of CBU0794, in J774A.1 macrophages, appears to be consistent at both 2 and 4 days post infection. The amount of gene expression in cell infection is similar to the amount seen when grown axenically in ACCM-2 medium. Since the time of performing this experiment, a separate microarray study [62] was published that analyzed the expression of the entire *C. burnetii* genome during infection of Vero cells. In this study, the authors compared gene levels at 5, 7, 14, and 21 days post infection, with day 3, serving as an early baseline. Interestingly, this study found that the levels of CBU0794 are higher early in infection and by 5 days are 1.5 fold decreased. This decreased level then stays throughout the remainder of infection. With these results, it would seem that CBU0794 is needed earlier during infection and then expression is dampened later when it is no longer needed. Because I used J774A.1 macrophages in

these experiments, it is impossible to look that late during infection. J774A.1 overgrow and die too quickly in a tissue culture dish which can limit our interpretations. Taken together these results lend credit to CBU0794's importance early in infection.

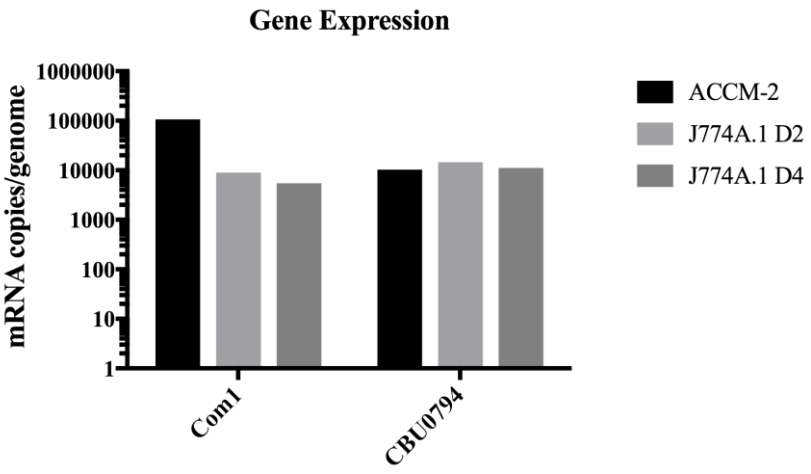

Figure 2.1. CBU0794 gene expression in infection and ACCM-2 growth shows constitutive levels. Quantitative PCR was done using gene specific primers for either Com1 or CBU0794. Graph shows number of mRNA copies per genome of *C. burnetii* present in either ACCM-2 growth cultures, or infected J774A.1 macrophages at either D2 or D4 post-infection.

The effector CBU0794 utilizes a nuclear localization sequence to traffic to the nucleus. Using bioinformatic analysis, we sought to identify the sequence required for the nuclear localization of CBU0794. Two different NLS domain algorithms,

NLStradamus [63] and cNLSmapper [64] each identified a unique potential NLS (Figure 2A). To test the contribution of these two domains on nuclear localization, we deleted each one individually and queried the nuclear localization of the generated CBU0794 alleles. Our results show that while NLS1 partially contributes to the nuclear localization, NLS2 is essential for CBU0794 to be directed to the nucleus. Moreover, this localization is dependent on the canonical nuclear import pathway. When the nuclear import receptor, Importin-β, is blocked with the pharmacological inhibitor Importazole, the nuclear localization of CBU0794 was inhibited, suggesting that this localization is dependent on the canonical receptor.

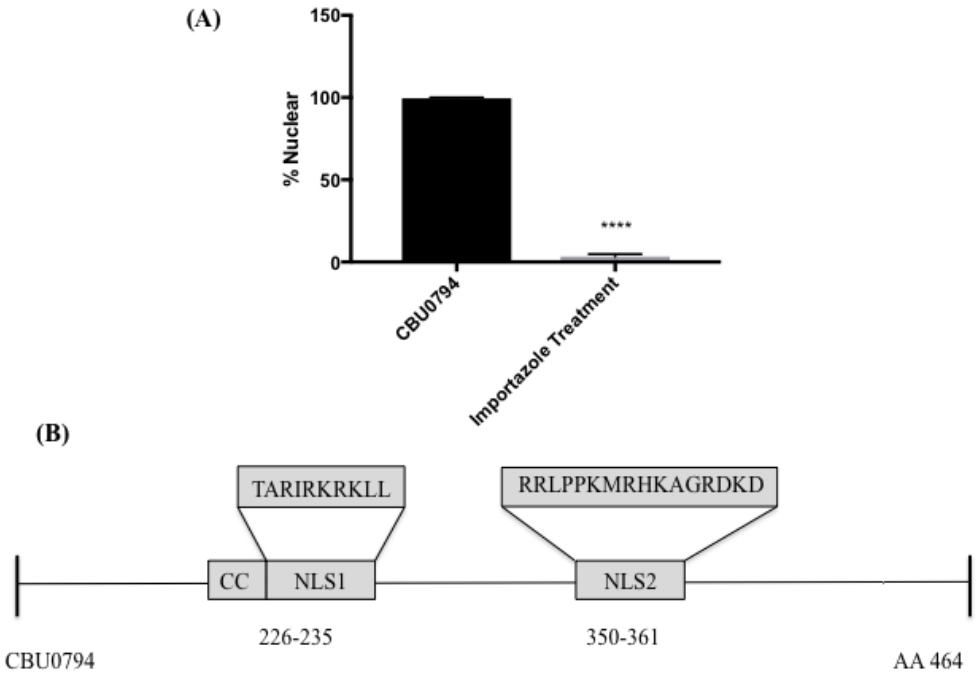

Figure 2.2. CBU0794 contains a canonical nuclear localization signal. Quantitation of Importazole treatment during transfection of CBU0794 in HeLa cells. Predicted nuclear localization signals present in CBU0794 according to bioinformatics analysis.

CBU0794 contains an essential nuclear localization sequence. To fully understand the essential elements for CBU0794's localization to the host cell nucleus, we individually deleted the two predicted nuclear localization sequences. The results, seen in Figure 3, were surprising. Deletion of the first predicted NLS partially contributed to the nuclear localization phenotype, about 50%. The second NLS, however, seemed to be more

responsible for the phenotype, as deletion of this region alone almost completely abolished the nuclear localization pattern. Alternately, it is possible given this result that deletion of these regions interfered with the protein structure enough to cause this phenotype.

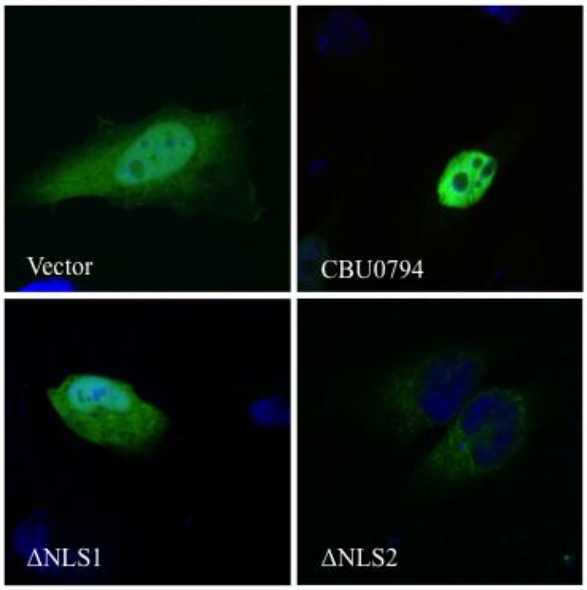

Figure 2.3. Contributions of predicted NLSs to CBU0794 nuclear localization. Confocal images of transfections of vector, full-length CBU0794, and deletion mutants from each predicted NLS. Images are representative from across at least three independent experiments.

Deletion of the coiled-coil region alters the stability of the protein. Using the bioinformatics prediction software SMRT, we also discovered that CBU0794 contains a predicted coiled-coil motif. A coiled-coil is a structural motif consisting of two to five helices forming a supercoil, often involved in protein interactions [65]. To understand the contribution of this region on protein functionality, we deleted the region encoding the coiled-coil sequence. The protein lacking a coiled-coil region appeared to be unable to localize to the nucleus during transient transfection. This may be due to instability of the protein when this region is absent. The central location of the coiled-coil domain, as well as the key role it plays on the folding of the protein, likely results in an unstable or misfolded protein. In localization studies using the ΔCC mutant, the protein appeared lightly punctate in the cytoplasm and was very faint. Given that it is a key structural element of this protein, deletion probably caused improper folding causing it to be degraded in the cytoplasm. This would correlate with the lower expression of this mutant and lack of nuclear translocation.

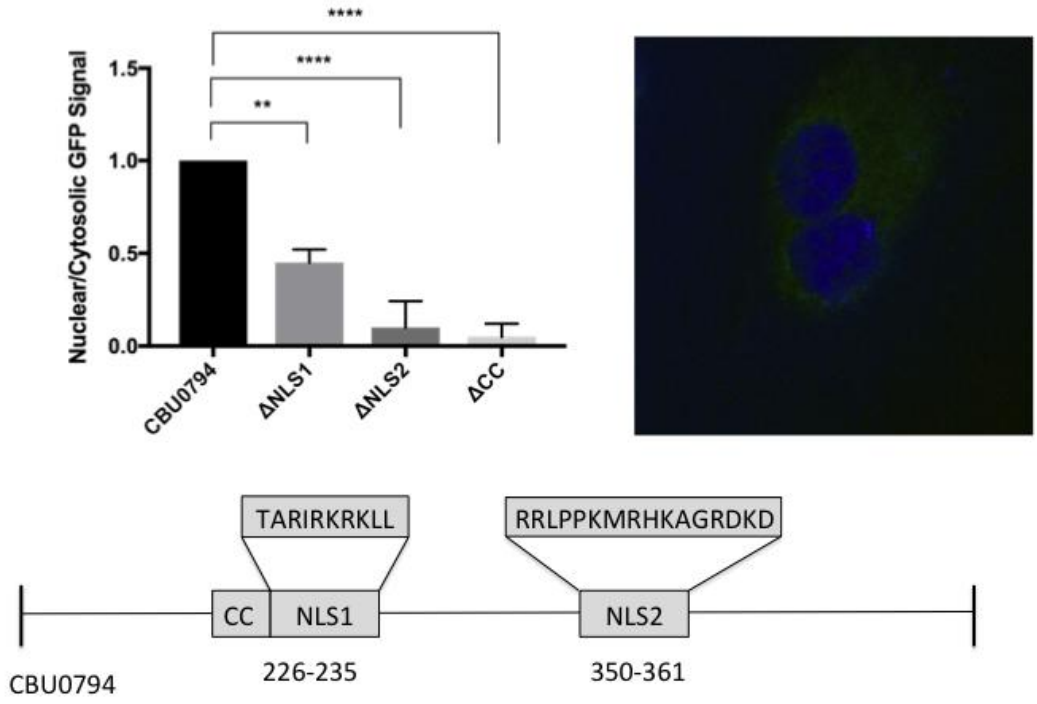

Figure 2.4. Deletion of the coiled-coil region of CBU0794 also prevents nuclear localization of the protein. Quantitation of deletions of NLS1, NLS2, and Coiled-coil region (CC) compared to full-length CBU0794. Confocal image shown is representative from across three independent experiments. **p<0.005, ****p<0.0001

EMAP analysis points to a role for CBU0794 in transcription. In order to understand functionality, CBU0794 was included in a collaborative Epistatis Miniarray profile

project (EMAP) [61]. EMAP uses *S. cerevisiae* to express a protein of interest, which is then mated to individual yeast mutants. The resulting data provides a profile of genetic interactions that are similar to the expression of the protein. Therefore, you can predict pathways that your protein may be involved to generate an impactful hypothesis.

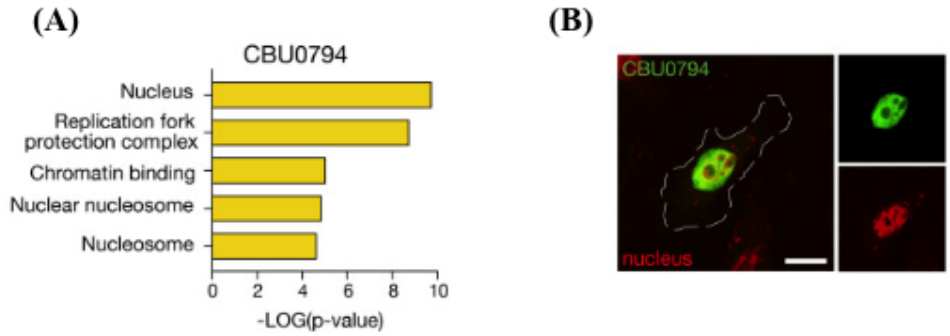

Figure 2.5. EMAP data analysis of CBU0794. (A) Enriched GO terms for significantly correlating genetic interaction profiles for CBU0794. (B) HeLa cells transiently transfected to express GFP-CBU0794, co-stained with Hoechst to visualize nuclei. Scale **Figure 2.5 cont.** bar, 10μm. **Figure adapted from Patrick and Wojcechowskyj, *et al.* (2018). *Cell Systems [61].***

In the case of CBU0794, the genetic interaction pathways, seen in Figure 2.5, supports an involvement with the nucleosome. The nucleosome is a term for a unit of DNA coiled around histones. This data shows that expression of CBU0794 correlates with mutants in chromatin or histone biology.

Mass Spectrometry Result
PARP1*
XRCC6/Ku70*
TBL1XR1*
XRCC5/Ku80
FACT complex subunit SUPT16H*
FACT complex subunit SSRP1
HDAC6

Table 2.3. Mass Spectrometry Results of CBU0794 Immunoprecipitation. Unique protein mass spectrometry for CBU0794-GFP pulldown listed in order of relative abundance. *Denotes testing by western blot with protein specific antibody.

CBU0794 interacts with TBL1XR1 *in vitro*. To assess protein interactions, we did a pulldown using GFP-tagged CBU0794 expressed in 293T cells. Mass spectrometry

analysis predicted several potential protein interactions with a subset of proteins involved in eukaryotic transcription (Table 2.3). It is interesting to note that all of the proteins from the mass spectrometry results listed in the table are nuclear proteins associated directly with DNA. Four of these seven proteins were tested by western blot to confirm protein interaction during CBU0794 pulldown. Confirmation of the mass spectrometry showed that CBU0794 does indeed interact with TBL1XR1, a key component of the SMRT/NCoR-HDAC3 complex (Figure 2.6). Protein interactions with other proteins tested could not be confirmed. Individual western blots probed for the other proteins on the list failed to confirm the mass spectrometry results (data not shown).

Transducin (β)-like X-linked receptor 1 (TBL1XR1) contains both a F-box as well as WD-40 repeats [66]. It is best characterized as a transcriptional activator for the SMRT/NCoR-HDAC3 repressor complex, regulating gene activation and repression. It participates in the complex by facilitating interaction with histones, with another protein TBL1, which was once thought to be functionally redundant with TBL1XR1 [67]. Interestingly, though they may share some functional redundancy, they also respond to individual upstream signaling [68]. Despite having a high degree of protein homology, their activities are regulated through differential phosphorylation [69].

TBL1XR1, through the SMRT/NCoR complex, is involved in regulating gene expression for multiple upstream signaling pathways including: activator protein-1 (AP-1), retinoic acid receptor (RAR), peroxisome proliferator-activated receptor γ (PPARγ), estrogen receptor (ER), thyroid hormone receptor (T_3R) and NF-κB, [70]. Mutations of

TBL1XR1 in human cells can result in numerous mental and physical developmental issues, including mental retardation and tumors [71].

TBL1XR1 can be present in both the cytoplasm or nucleus [68] but the CBU0794 interaction appears to occur in the nucleus. The interaction of CBU0794 and TBL1XR1 is dependent on the nuclear localization of CBU0794, as deletion of the NLS abolished this interaction. When we repeated the pulldown with the NLS mutant that does not go to the nucleus, the interaction with TBL1XR1 is no longer present. We can hypothesize that this protein interaction occurs after CBU0794 enters the nucleus since the NLS mutant doesn't interact with TBL1XR1. It could be, however, that just the deletion of the NLS region of CBU0794 abolishes the binding interaction.

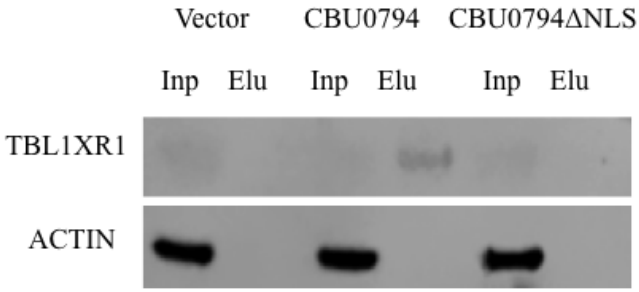

Figure 2.6. Western blot confirmation of CBU0794 immunoprecipitation confirms interaction with TBL1XR1. Input and Elution of GFP immunoprecipitation for

Figure 2.6 cont. pEGFPC1 vector, CBU0794 and CBU0794ΔNLS was subjected to a western blot using a TBL1XR1-specific antibody (Sigma). Actin was used as a loading control.

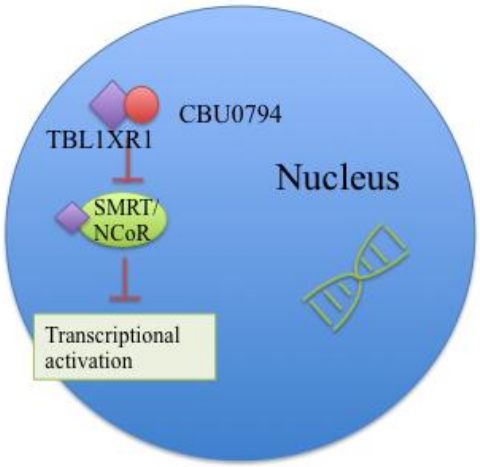

Figure 2.7. Hypothesis for implications of CBU0794 and TBL1XR1 interaction. Our primary hypothesis to test was one in which CBU0794 interacts with TBL1XR1 to prevent activation of transcription through the SMRT/NCoR complex.

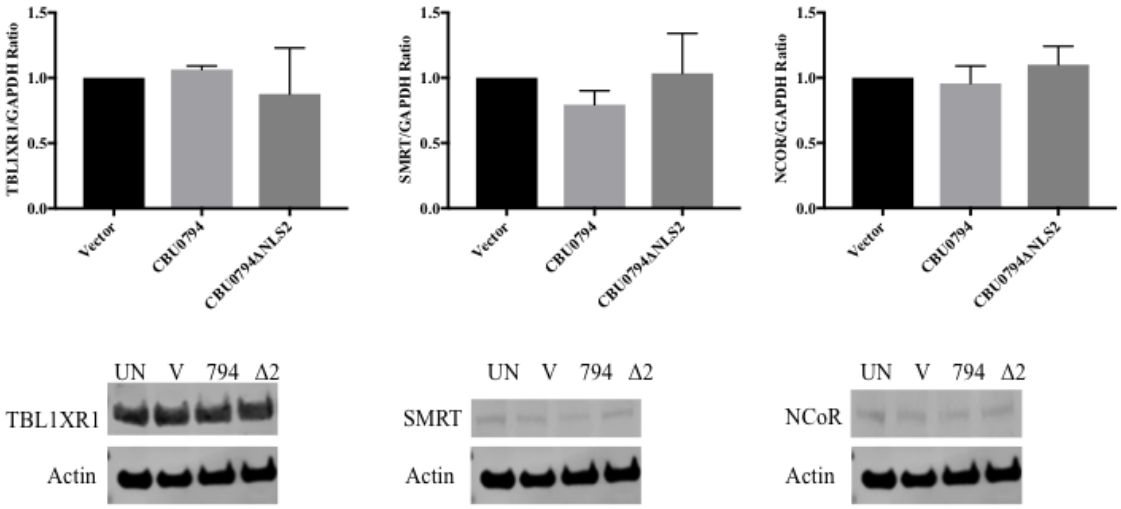

Figure 2.8. Expression of CBU0794 Does Not Effect Transcription or Protein Levels of the SMRT/NCoR Complex. (A) Gene expression analysis in 293T cells during transfection conditions with respective constructs. Graphs are mean + SD of three independent experiments. (B) Representative graphs of western blot analysis in 293T cells during transfection. UN = untransfected.

Interaction of CBU0794 and TBL1XR1 does not alter gene expression or protein levels of the SMRT/NCoR complex components. Because TBL1XR1 is involved in multiple transcriptional pathways, follow-up analysis proved to be difficult. The first step in evaluating CBU0794's effect of the SMRT/NCoR pathway was to look at its effect on protein levels of core components of this pathway. To do this, we expressed

CBU0794 and the NLS mutant in 293T cells, as done in previous protein interaction studies. We then analyzed protein levels of TBL1XR1, SMRT, and NCoR in these cells. As seen in Figure 2.8, there did not appear to be a significant difference in expression of the protein of interest when CBU0794 was expressed compared to vector or untreated cells. There was also no change in transcript levels of these genes under the same conditions.

In addition to its crucial role in the SMRT/NCorR pathway, TBL1XR1 has been shown to be important for transcription through the Wnt-β-catenin signaling pathway [72]. The Wnt/β-catenin pathway is involved in many cellular processes such as development, stem cell proliferation and tumorigenesis [73]. It has been shown that TBL1XR1 is SUMOylated as a result of upstream Wnt signaling, thus removing the protein from the SMRT/NCoR complex. It then forms a new TBL1XR1-TBL1-β-catenin complex causing transcriptional activation of Wnt-regulated genes [74]. Although there is no evidence of modulation of the Wnt/β-catenin pathway during infection by *C. burnetii*, it has been demonstrated by a number of other bacteria, including *E. chaffeensis* and *M. tuberculosis* [75, 76].

We hypothesized that CBU0794 causes SUMOylation of TBL1XR1 in the absence of Wnt signaling to dissociate it from the SMRT/NCoR pathway. This could be either direct or indirect post-translational modification in the presence of CBU0794. Interestingly, when we compared cell lysates by western blot we observe a small population of protein reacting with the TBL1XR1-specific antibody that is shifted to a higher molecular weight (Figure 2.9). Because most TBL1XR1 migrated at the correct

size, this modification occurs in a minority of the TBL1XR1 population. Importantly, though, this band only appears when CBU0794 is expressed; both vector and CBU0794 ΔNLS do not show this higher molecular weight species.

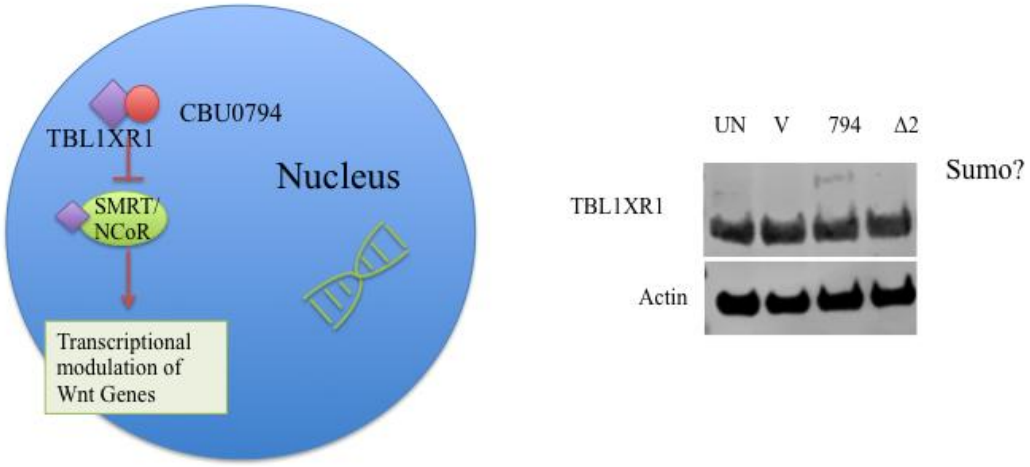

Figure 2.9. Potential model of CBU0794 and TBL1XR1 involved in Wnt signaling. (A) Hypothesized model by which interaction of TBL1XR1 and CBU0794 cause an impact on Wnt gene transcription. (B) Western blot of TBL1XR1 in transfection

Figure 2.9 cont. conditions show a small fraction of TBL1XR1 that has been modified in the presence of CBU0794.

Further testing must be done to determine if this is a result of SUMOylation or some other post-translational modification. TBL1XR1 can be post-translationally

modified in other ways, including phosphorylation [69]. We also lacked a positive control to show SUMOylation of TBL1XR1.

Expression of CBU0794 alone does not appear to change transcriptional levels of any host proteins. In order to assess whether or not CBU0794 has an effect on global transcription, we performed an RNA-seq in 293T cells. We compared transcriptional profiles of vector, CBU0794 and CBU0794 ΔNLS transfected cells. A mock-transfected sample was also used for additional baseline comparison. Each condition was performed in triplicate. The heat map of transcriptional changes (Figure 2.10) indicated that there is not a lot of variation among transcript levels. The largest difference is a transcriptional variance between mock and GFP vector transfected cells. Sample N252 is the CBU0794ΔNLS.

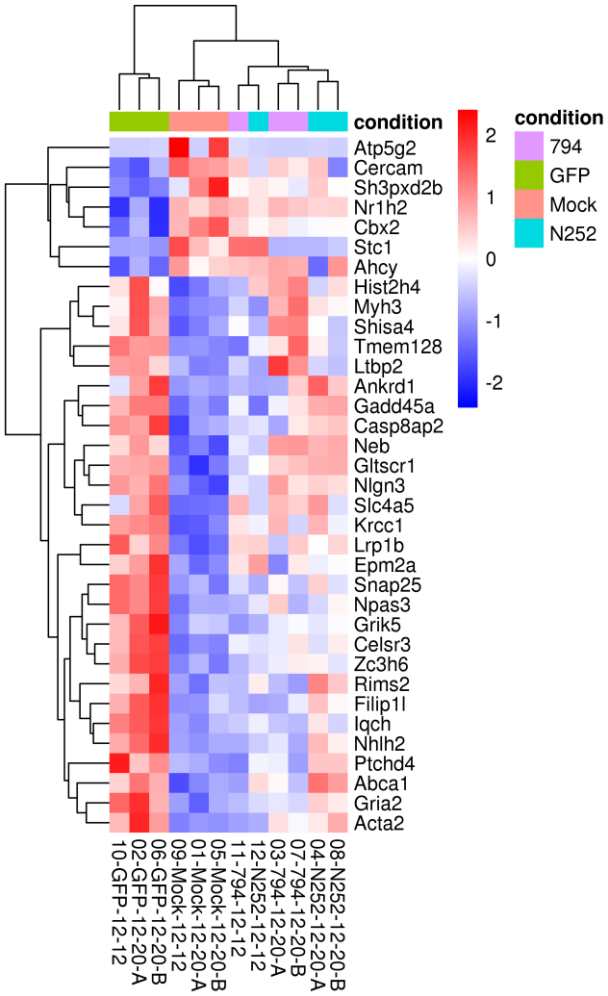

Figure 2.10. Heat map of RNA-seq of all three replicates showing fold-change of differentially expressed transcripts in each sample. RNA-seq samples were analyzed for a 2-fold change in transcription levels. Each condition was done in triplicate in individual experiments. Each replicate is plotted individually.

Additionally, looking at a Venn diagram (Figure 2.11) of up- and down-regulated genes that have at least a 2-fold change, there not a significant difference between samples. Only 5 genes are up-regulated in response to CBU0794 expression. There are 15 genes are down-regulated under CBU0794 expression conditions, with an additional 9 genes also down-regulated during the mock transfection. From this data, it is difficult to conclude whether there is an active transcriptional response induced by transfection of CBU0794. Follow up of individual genes is needed.

(A) **(B)**

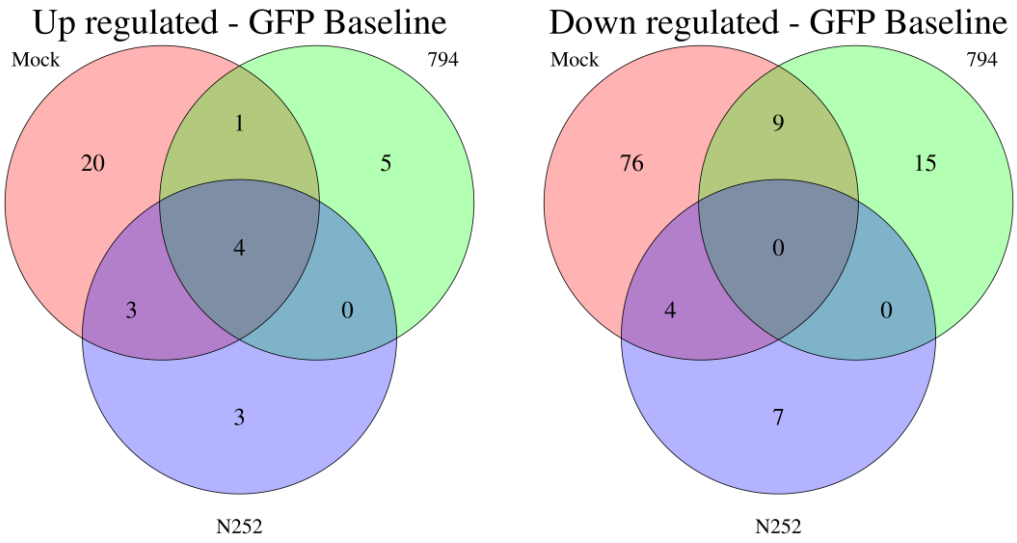

Figure 2.11. Venn diagram of RNA-seq showing differentially expressed transcripts either up-regulated (A) or down-regulated (B), using the GFP sample as a baseline.

The biggest caveat to this experiment is that we tested transfection conditions instead of infection. The lack of a CBU0794 mutant strain prevents an infection-based comparison. Although we did not observe transcriptional differences in our experiment, that does not suggest that CBU0794 is not involved in transcriptional modulation. We did the RNA-seq under normal transfection conditions. We may have needed an external stimulus to be present in order to induce any transcriptional modulation.

Discussion

A growing body of literature has highlighted the importance of Nucleomodulins, bacterial proteins that interfere with host nuclear processes [48]. While previous observations have revealed six potential *C. burnetii* nucleomodulins, this is the first in depth analysis to characterize an effector with nucleomodulin activity.

Protein interaction analysis predicted that CBU0794 interacts with the eukaryotic transcriptional regulator TBL1XR1 in the host cell's nucleus. Therefore, we propose a model where upon infection by *C. burnetii*, the Type IV secretion machinery is activated and secretes CBU0794 into the host cell. Using canonical nuclear import, CBU0794 traffics into the host nucleus where it interacts with its protein partner TBL1XR1. This interaction was confirmed by western blot analysis. Co-localization studies between CBU0794 and TBL1XR1 could further validate this finding. Consequences of this interaction are yet to be determined, but it could have wide reaching effects on host transcription in response to upstream signaling events.

We showed that CBU0794 interacts with the regulator protein TBL1XR1. This protein is involved in multiple transcriptional responses, all of which require an extracellular stimulus. If CBU0794 were indeed interacting with TBL1XR1 to manipulate this transcriptional response, you wouldn't see an effect without the stimulus being present. In normal cellular conditions, TBL1XR1 is bound as a repressor to the SMRT/NCoR complex. The addition of a nuclear hormone receptor causes a conformational change that removes TBL1XR1 from the SMR/NCoR complex allowing transcription to occur.

Future studies will focus on the impact of CBU0794 on pathogenesis of *C. burnetii*. Despite the DNA sequence of CBU0794 being very AT-rich, transposon mutagenesis has failed to produce a CBU0794 mutant. This may be due to an essential functionality of this protein for the viability of the organism. More likely, a mutant could be made non-viable due to its location among essential t-RNAs in the *C. burnetii* genome. A more targeted approach needs to be done to make a site-directed CBU0794 mutant, which will determine if this mutant would be viable. With this mutant, we can further assess the contribution of CBU0794 to pathogenesis in both intracellular studies as well as a mouse model. A CBU0794 mutant will also allow us to further study the transcriptional modulation as a result of its interaction with TBL1XR1.

CHAPTER III

NUCLEAR TRANSLOCATION OF *COXIELLA BURNETII* T4SS EFFECTOR CBU0388 IS REQUIRED FOR PATHOGENESIS

Synopsis

Coxiella burnetii is a Gram negative, obligate intracellular pathogen and the causative agent of the zoonotic disease Q fever. This organism utilizes an essential type IVB secretion system (T4BSS) to translocate effector proteins into the host cell to promote its own intracellular survival and replication. To date, over 100 effector proteins have been identified but not much is known about their functionality. Here we demonstrate the nuclear trafficking of one such effector, CBU0388, which is essential for replication of *C. burnetii* both *in vitro* and *in vivo.* Trafficking both in and out of the nucleus appear to be important for its mechanism of action within the host cell. We show that this trafficking is dependent on both a nuclear localization signal (NLS) and a nuclear export signal [49]. This is the first instance of a nuclear-localized effector required for pathogenesis in *C. burnetii.*

Introduction

Coxiella burnetti is a gram-negative obligate intracellular pathogen and the causative agent of Q fever, a zoonotic disease transmitted from aerosols of infected livestock. Because of its low infectious dose, environmental stability, and aerosol route of transmission, *C. burnetti* is classified as a category B select agent. While *C. burnetii* primarily infects alveolar macrophages after inhalation, it is capable of infecting a

variety of host cells, including phagocytic and non-phagocytic cells. Once inside the cell, the bacteria set up a replicative niche called the *Coxiella*-containing vacuole (CCV) where they need an acidic pH in order to promote replication. C. *burnetii* utilizes a Dot/Icm secretion system to deliver over 100 effectors into the host cell, creating a unique replicative niche for itself. Remodeling of the CCV is essential for survival of *C. burnetii* inside a hostile lysosome-like compartment.

Several bioinformatics and functional screens have been performed by our lab and others to identify potential secreted effector proteins [31, 42, 77]. To date, over 100 T4SS effectors have been described for the virulent Nine Mile strain of *C. burnetii*. With only a handful of effectors having been characterized so far, there is a huge gap in knowledge to understand how *C. burnetii* modulates its host environment to survive.

Here, we describe one effector, CBU0388, which is necessary for CCV biogenesis and replication. In addition, it appears to be required for *in vivo* pathogenesis of the organism in a SCID mouse model of infection. Once secreted into the cytoplasm, CBU0388 traffics through the host nucleus using both a canonical nuclear localization signal and nuclear export signal.

Materials and Methods

Cell Lines and Strains. Strains used in this study are listed in Table 3.2. *C. burnetii* Nine Mile phase II (strain RSA439, clone 4). HeLa cells were used for all the transfection experiments.

Cloning and Plasmids. Bioinformatic predictions of nuclear localization signals were generated using cNLSmapper (http//nls-mapper.iab.keio.ac.jp/) and/or NLStradamus

(http://www.moseslab.csb.utoronto.ca/NLStradamus/). Nuclear export signals were identified through the online bioinformatics tool NetNES 1.1 Server (http://www.cbs.dtu.dk/services/NetNES/).

Transformation and Growth of *C. burnetii.* *C. burnetii* was axenically cultured in ACCM-2 media as previously described [40]. Competent cells were made my spinning down and washing in sterile water with 10% glycerol. For transformation, *C. burnetii* was resuspended with sterile water before electroporation with 10-20ug of plasmid at 1800V, 400Ω in a 0.2cm cuvette. Where appropriate, 350 μg/mL of kanamycin or 5 μg/mL of chloramphenicol was added for selection. For anhydrotetracycline induction, 50 ng/mL was added for 24 hours as done previously [78].

Cell transfection and Inhibitor Treatment. For ectopic expression in mammalian cells, HeLa cells (ATCC) were seeded at 60% confluence in a 24-well plate. The following day, cells were transiently transfected with Lipofectamine 3000 according to manufacturer's protocol. For treatment with Importazole (Sigma-Aldrich), cells were transfected for eleven hours following addition of 10μM for 1 hour before fixing. For Leptomycin B (InvivoGen) treatment, cells were transiently transfected for 8 hours before addition of 50nM to each well for 4 hours.

Fluorescence Microscopy. At indicated timepoints, cells were fixed with 4% Paraformaldehyde in PBS at room temperature for 10-15 minutes. After fixation, cells were rinsed in PBS and quenched with 50mM ammonium acetate at room temperature for 10 minutes. Coverslips were then incubated in blocking buffer (0.02% Saponin in PBS with 10% horse serum) for 30 minutes in the dark. After blocking, the coverslips

were incubated with primary antibody diluted in blocking buffer for 1hr at room temperature in the dark. Coverslips were then rinsed and incubated for another hour with secondary antibody. To visualize the nucleus, coverslips were stained with Hoescht in water for 10 minutes before a final wash with water. Coverslips were mounted on slides with Mowiol and imaged with a Nikon A1 confocal microscope. The Nikon elements software was used for image analysis and quantification.

Western Blotting, Cell Fractionation, and Immunoprecipitation. Immunoblots were performed using anti-HA high affinity rat monoclonal antibody (Roche; 3F10). Goat monoclonal anti-rat (LICOR) and goat monoclonal anti-mouse (LICOR) were used at dilutions of 1:10000.

***C. burnetii* Growth Curves.** Bone marrow derived macrophages were acquired from BL6 mice as described (paper reference). SCID mouse infection were done as published previously [34]. HeLa cells were seeded in 24-well plates at a density of 5×10^4 per well. The following day, the indicated strains of *C. burnetii* were used to infect at a MOI of 50. The MOI was calculated using the Quanti-iT PicoGreen dsDNA Assay kit (Life Technologies). Cells were centrifuged at 500xg for 10 minutes before placing in the 37°C incubator for one hour. After incubation, the cells were washed three times and the media was replaced with DMEM with 10% FBS. At day 1, 4, and 7, cells were lysed in DNA lysis buffer (1M Tris, 0.5M EDTA, Lysozyme, Glucose) with Proteinase K. Genomic DNA isolated from the samples using the Roche High Pure PCR Template Prep kit (Indianapolis, IN) according to the manufacturer's protocol. Resulting genomic

DNA was quantified through qPCR specific for either the *IS1111* insertion sequence or Himar transposon as described previously [34].

Statistical Analyses. Statistical analysis was performed with Prism (GraphPad Software, Inc.) using an unpaired, Student's t-test. *P<0.05, **P<0.01.

Table 3.1. Oligonucleotides used in this study

Oligonucleotide	Oligonucleotide Sequence (5'-3')	Application
388 NLS1del 1F	GTCCGGACTCAGATCTATGAGATCAT GGTTGTCGTT	Infusion
388 NLS1del 1R	CGTCATCATTGCTGACTGGTTTTTTTA CCCACAAAT	
388 NLS1del 2F	TCAGCAATGATGACGACATT	
388 NLS1del 2R	CCGCGGTACCGTCGACTTAGCTTTTTTC AAAATTTACTTT	
388 NLS2del 1F	GTCCGGACTCAGATCTCCAGATCTTTGTCGTTAC AAGCTATTGAGAAACT	
388 NLS2del 1R	AACCTTTTGAAAAATATTTCATTTTGCG CAGAATAAA	
388 NLS2del 2F	ATTTTTCAAAAGGTTAAAGGTG	

Table 3.1. Oligonucleotides used in this study continued

Oligonucleotide	Oligonucleotide Sequence (5'-3')	Application
388 NLS2del 2R	CCGCGGTACCGTCGACCCGTCGACGCTTTTTTC AAAATTTACTTTACGCT	
388 NLS3del 1F	GTCCGGACTCAGATCTCCAGATCTTTGTC GTTACAAGCTATTGAGAAACT	
388 NLS3del 1R	CTTGAGCTCGAGATCTCATTTTTATTGTTTTA AGCTCCACATC	
388 NLS3del 2F	GAATTCTGCAGTCGACTCAGAAAATCTCGTTAA TCTTCCAC	
388 NLS3del 2R	CCGCGGTACCGTCGACCCGTCGACGCTTTTTTCA AAATTTACTTTACGCT	
388 Tn7in F	ATTTACGCGTGAATTCATGAGATCATGGTTGTCGTT	
388 Tn7in R	GCTTCTCGAGGAATTCTTAGCTTTTTTCAAAATTTACTTT	
388 cDNA primer	GTTTGAATTTCCGCTTGATTCTTATTTTTTCC	
388 cDNA F	TGAGATCATGGTTGTCGTTACA	
388 cDNA R	TTTGAATTTCCGCTTGATTCTT	
ObgE cDNA F	AAGTCCACCTTCATCCATGC	
ObgE cDNA R	CGCTAGCGCCTTAATTAAC	
rpmA cDNA F	CTTGCGGGGAATATCATTGT	

Table 3.1. Oligonucleotides used in this study continued

Oligonucleotide	Oligonucleotide Sequence (5'-3')	Application
rpmA cDNA R	CGGCTCAATGGAGACAAAGT	
rplU cDNA F	GAGAAGTTGGCGCAAGATGT	
rplU cDNA R	TGCCGTTTCATGTGATGTTT	
cDNA up2 F	CTTCGCTTCATACGGGCTAC	
cDNA up2 R	CCTCCCCATTGAATCTCTCA	
cDNA up1 F	CCAACCGAGTTCGAAACAAT	
cDNA up1 R	CGTATATGGACCCACCCTTG	
AA912-39 1F	GTCCGGACTCAGATCTCCAGATCTTTGTCG	Deletion
	TTACAAGCTATTGAGAAACT	of NLS3
AA912-39 1R	CTTGAGCTCGAGATCTCATTTTTAT	
	TGTTTTAAGCTCCACATC	
AA912-39 2F	GAATTCTGCAGTCGACTCAGAAAATCT	
	CGTTAATCTTCCAC	
AA912-39 2R	CCGCGGTACCGTCGACCCGTCGACGCTTT	
	TTTCAAAATTTACTTTACGCT	
mCDK1 F	AGAAGGTACTTACGGTGTGGT	
mCDK1 R	GAGAGATTTCCCGAATTGCAGT	
mActin F	CGCCACCAGTTCGCCATGGA	

Table 3.1. Oligonucleotides used in this study continued

Oligonucleotide	Oligonucleotide Sequence (5'-3')	Application
mActin R	TACAGCCCGGGGAGCATCGT	

Table 3.2. Bacterial strains and plasmids used in this study

Strain or Plasmid	Description	Source
Strains		
E. coli DH5α	F– Φ80*lac*ZΔM15 Δ(*lac*ZYA-*arg*F) U169 *rec*A1 *end*A1 *hsd*R17 (rK–, mK+) *pho*A *sup*E44 λ– *thi*-1 *gyr*A96 *rel*A1	Stratagene

Table 3.2. Bacterial strains and plasmids used in this study continued

Strain or Plasmid	Description	Source
E. coli Stellar Cells	F–, endA1, supE44, thi-1, recA1, relA1 gyrA96, phoA, Φ80□ lacZΔ M15, ΔmcrA, λ– Δ(lacZYA - argF) U169, Δ(mrr - hsdRMS - mcrBC)	Clontech

Table 3.2. Bacterial strains and plasmids used in this study continued

Strain or Plasmid	Description	Source
C. burnetii Nine Mile (RSA439)	Phase II, Clone 4	
RSA439 MK DotA::Tn, Cm^r		
RSA439 MK CBU0388::Tn, Cm^r		
Plasmids		
pEGFP-C1	C-terminal fusion to EGFP, Kan^r	Clontech
pEGFP-C1 0388	CBU0388 cloned into pEGFP-C1	[31]
pEGFP-C1 0388Δ NES	CBU0388Δ NES cloned into pEGFP-C1	this study
pEGFP-C1 0388 ΔNLS	CBU0388Δ NLS cloned into pEGFP-C1	this study
pST100	pUCR6K-miniTn7-Kan-TetRA-4xHA Anhydrotetracycline-inducible expression cassette of 4xHA in the miniTn7-Kan transposon sequence-	[46]
pST101	CBU0388 cloned into pST100	this study

The effector CBU0388 is required for intracellular replication in multiple *in vitro* cell types. We previously described a transposon mutant in *CBU0388* as having an attenuated growth in J774A.1 macrophages [31]. Here, we show that the CBU0388 mutant is unable to replicate in any host cell, including macrophages and HeLa cells (Figure 3.1). In tissue culture cell infection with the CBU0388::tn mutant, *C. burnetii* cannot form an expansive vacuole, but instead is restricted in a tight vacuole where it cannot replicate. Thus, this protein might be important for vacuole biogenesis.

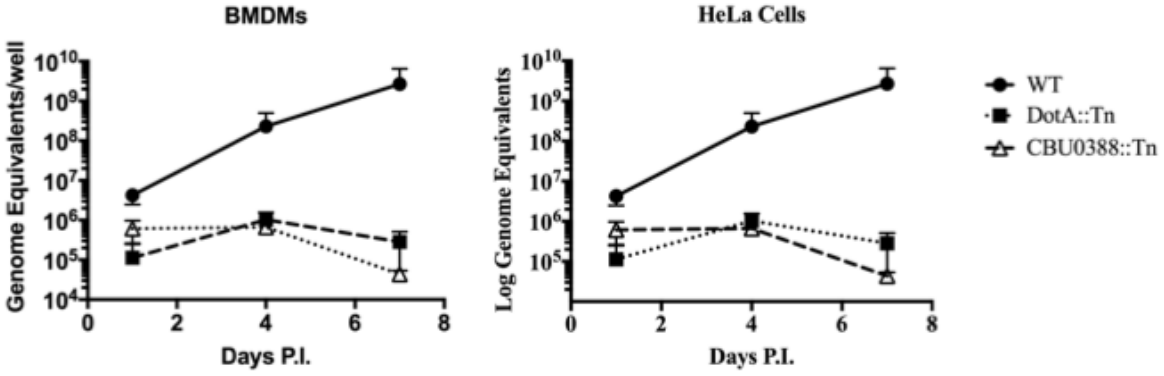

Figure 3.1. CBU0388 appears to be necessary for *C. burnetii* replication in tissue culture cells. BMDMs or HeLa cells were infected with NMII, *DotA*::Tn, *Cbu0388*::Tn or *CBU0388*::Tn Comp and lysed for genome equivalents on D1, D4 and D7. Values are

Figure 3.1 cont. mean ±SD of triplicate experiments. Data was analyzed using a One-way ANOVA with Prism GraphPad. * P<0.05 **P<0.005, *** P<0.0001. Error bars are mean ±SD.

CBU0388 is important for pathogenesis *in vivo* using a SCID mouse model. Using a SCID mouse model, the bacterial load at 10 days post-infection is significantly reduced in the CBU0388::tn mutant compared to wild type (Figure 3.2). The CBU0388::tn also cannot cause splenomegaly, a hallmark for productive pathogenesis in a SCID mouse model of *C. burnetii* infection [34]. This attenuation further suggests the important role that CBU0388 must play during *in vivo* infection.

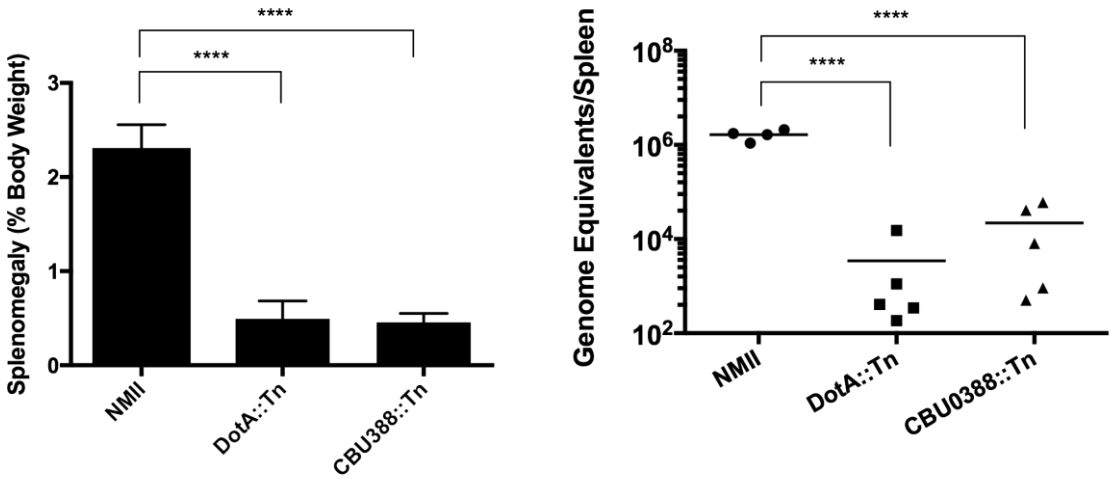

Figure 3.2. CBU0388 is required in *vivo* pathogenesis in a SCID mouse model. (A) Genome equivalents calculated by qPCR from DNA purified from spleens at day 10 post-infection (B) Splenomegaly for SCID mouse infection at day 10 post-infection calculated as spleen weight as a percentage of total body weight at the time of necropsy. Error bars are mean ±SD. Asterisks represent statistically significant reductions in genome copies (A) or spleen weight (B) when compared to wildtype NMII infection (****P< 0.0001) calculated by One-Way ANOVA with Dunnet's Multiple Comparisons test.

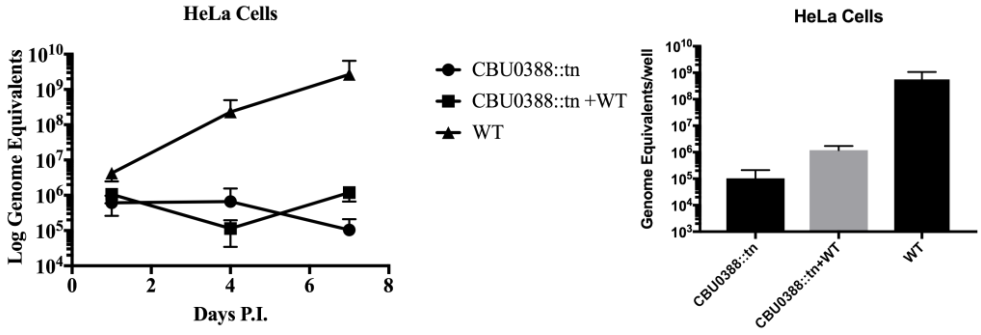

Figure 3.3. Complementation was not achieved through *trans*-complementation in HeLa cells. (A) Growth curve of *C. burnetii* strains in HeLa cells. The CBU0388::tn mutant was detected using a probe specific to the Himar1 in order to differentiate it from the WT bacteria. (B) Genome equivalents for each strain at 7 days post infection showing a modest growth of 1 log compared to CBU0388::tn alone, but not significant compared to the WT strain.

The effector CBU0388 may contribute to acute virulence. CBU0388 was an interesting protein to study for many reasons. Though we already had a transposon mutant showing a growth defect, we knew nothing about the protein itself. In order to understand more about the potential functionality of this protein, we looked at the *C. burnetii* genome itself. As seen in Figure 3.4, the first remarkable feature of this gene encoding CBU0388 is its size. At greater than four thousand base pairs in length, this is the largest T4SS substrate in the genome. The protein encoded by this gene is 161 kDa in size, well over the normal size of other *C. burnetii* substrates, which averages at only

33 kDa. Evolutionary selection would indicate that given its size, CBU0388 must be important to *C. burnetii* for it to keep it in the acute Nine Mile strain.

ORF	Size	Function
rplU	353bp	50S ribosomal protein L21
rpmA	272bp	50S ribosomal protein L27
obgE	1019bp	GTPase
CBU0388	4179bp	Hypothetical protein
rpsT	272bp	30S ribosomal protein S20
mviN	1547bp	Virulence factor
ribF	1037bp	FMN adenylyltransferase

Figure 3.4. Depiction of the *C. burnetii* genome showing the genomic locus that includes CBU0388.

One idea we wanted to explore further was whether or not CBU0388 was conserved throughout strains of *C. burnetii.* Strains of *C. burnetii* are classified largely by their ability to cause either acute or chronic infections. We compared the genomic integrity of the CBU0388 coding region in selected strains to determine whether CBU0388 was conserved across broad classes of these strains. The conservation status of CBU0388 is shown in Figure 3.5. From the figure, you can clearly see that the full length CBU0388 is not present in the Dugway strain, K strain, or G strain, all of which do not cause acute disease. In fact, the only strains where CBU0388 was fully intact and coding was Nine Mile and Henzerling, another acute disease isolate. In both the Dugway and K strains, internal deletions cause frameshift mutations resulting in two separate potentially coding regions. In the G strain, bioinformatics analysis predicts the same one open reading frame in the acute isolates. Looking at the genomic sequences, however, you see there are actually fourteen nucleotide changes that result in multiple frameshifts. While there are also numerous changes to the genome in these chronic isolates compared to the Nine Mile strain, we hypothesize that CBU0388 may contribute to acute virulence since it is only found in full-length form in strains that cause acute disease. The only way to test this would be to complement these chronic isolates with a fully coding CBU0388 to see if there is any effect on their ability to cause acute disease. There are also likely a larger number of proteins that contribute to acute virulence than just CBU0388, so you may not see any noticeable difference with adding just this one to those strains. This must be tested to know for sure.

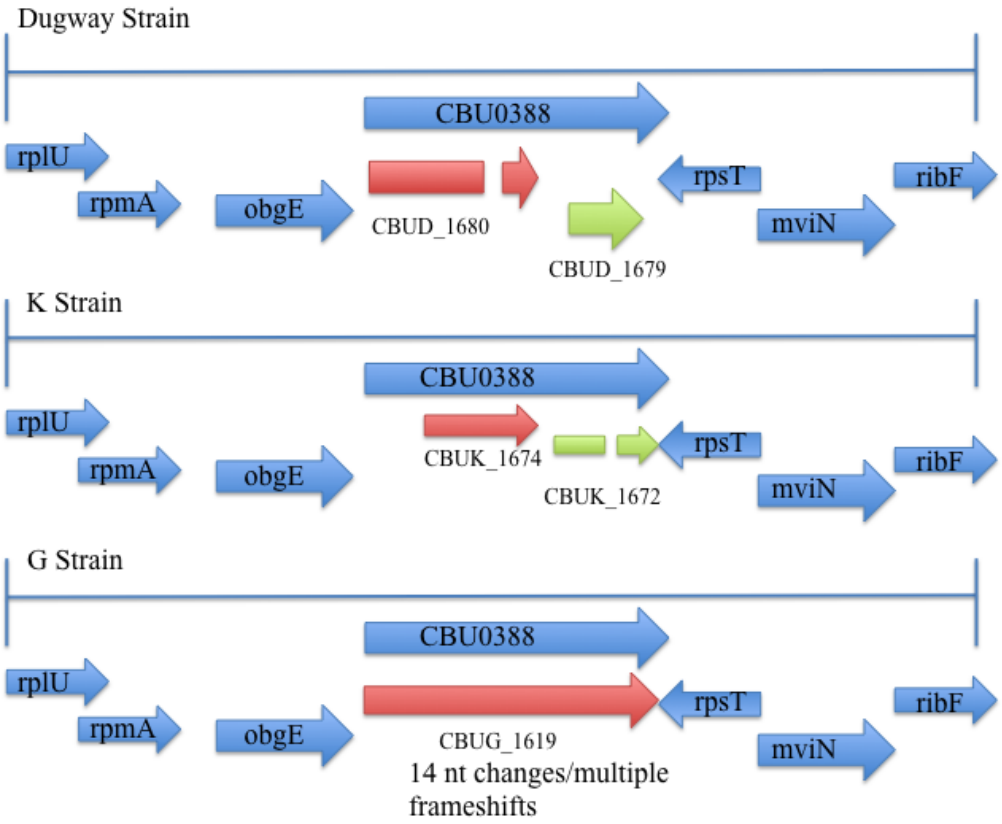

Figure 3.5. Conservation of CBU0388 across other *C. burnetii* strains. Comparison on genome annotation of NMII (blue) with three different chronic strain isolates.

Gene expression of CBU0388 is expressed throughout infection. Previous screening studies by our lab predicted CBU0388 as potentially regulated by the two component system PmrA/B based on upstream sequence homology [30]. A previous paper showed the PmrA/B controls gene expression of 43 different genes in *L. pneumophila* using a consensus sequence for binding [79]. That same study also showed the PmrA/B system regulated dot/icm genes in *C. burnetii*. We tested the expression of CBU0388 during

axenic growth as well as during infection (see Figure 3.6). CBU0388 appears to be stably expressed during infection. The expression level during infection is lower than compared to axenic growth. This data was further confirmed by a microarray showing a stable expression level of CBU0388 at day 3, 5, 7, 14, and 21 of infection in vero cells [62].

Given its location in the genome, it was unclear if CBU0388 is the last gene in an operon. Since the transposon insertion is at the end of the CBU0388 sequence, there is not a high probability of polarity causing the growth phenotype. But if the gene was in an operon, it could give us more information about the regulation and importance of the gene. We initially tried to identify a promoter upstream of CBU0388 by sequence verification and investigate it further through 5' race analysis. During this process, however, a microarray data set was published and showed differential expression of the upstream genes *rplu*, *rpmA*, and *obgE*, eliminating the hypothesis that CBU0388 was co-regulated with these genes [62]. While CBU0388 expression was stable throughout long-term infection, *rplu*, *rpmA*, and *obgE* expression was higher initially and decreased at later timepoints.

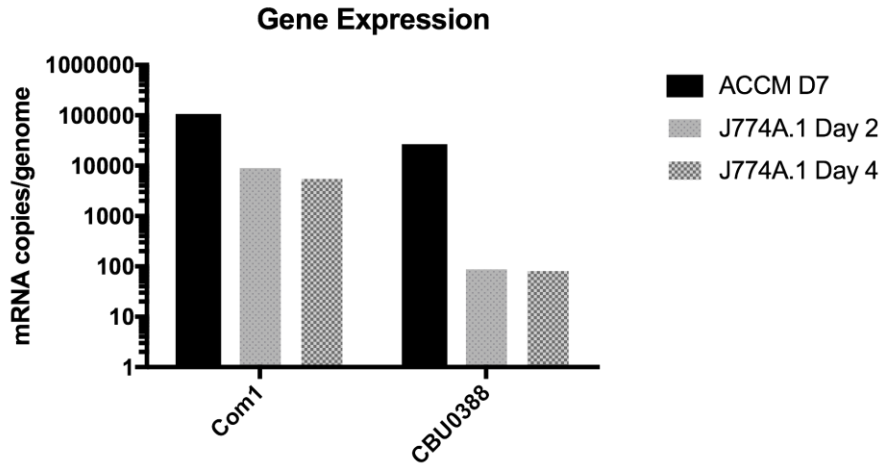

Figure 3.6. CBU0388 is expressed throughout infection in J774A.1 macrophages. Growth curve analysis was done to determine the expression level of CBU0388 both during axenic growth in ACCM-2 media and during J774A.1 macrophage infection at day 2 and day 4 post-infection. Com1 was used as a control for a gene that is constitutively expressed by *C. burnetii*. Graph shows one representative experiment with three technical replicates.

Nuclear localization and export signals are required for CBU0388 trafficking to the host nucleus. Based on our previous observation that CBU0388 is nuclear-localized during ectopic expression [31], we hypothesized that CBU0388 uses a NLS to traffic into the nucleus of host cells. To test this, we used the pharmacological inhibitor Importazole (IPZ), which inhibits the nuclear import receptor Importin B. In CBU0388-transfected cells treated with Importazole, the protein cannot enter the nucleus and is

seen only in the cytoplasm. This suggested that CBU0388 uses the canonical nuclear import pathway, which would be dependent on a NLS. We used NLStradamus to bioinformatically screen for a canonical nuclear localization signal [64]. Using this online prediction algorithm, we identified three potential nuclear localization signals in the amino acid sequence of CBU0388 (Figure 3.7). A canonical nuclear localization signal is composed of a series of basic amino acids which cause the protein to fold in a manner to form a binding pocket for the import adapter protein Importin α. A NLS can be either monopartite or bipartite, which contains a linker. To test their contribution to nuclear localization, we deleted each predicted NLS and transfected each resulting construct into HeLa cells to assess their nuclear translocation. We found that only one of the predicted NLSs were fully functional for translocation into the nucleus of the host cell (Figure 3.8). Deleting this NLS prevents the protein from entering the nucleus, so localization is restricted to the cytoplasm.

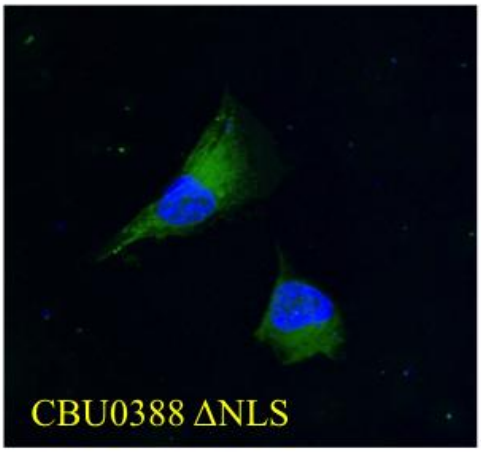

	Predicted Sequence	Cannonical Sequence
NLS	SLYHHRGKRRF	Monopartite: K (K/R)X(K/R) Bipartite: $(K/R)(K/R)X_{10\text{-}12}\ (K/R)_{3/5}$

Figure 3.7. CBU0388's nuclear localization is dependent on a cannoncial nuclear localization signal. Confocal image of HeLa cells transfected with the pEGFP CBU0388 ΔNLS plasmid. Shown above is one representative image from at least three independent experiments. The NLS amino acid sequence matches a canonical monopartite sequence.

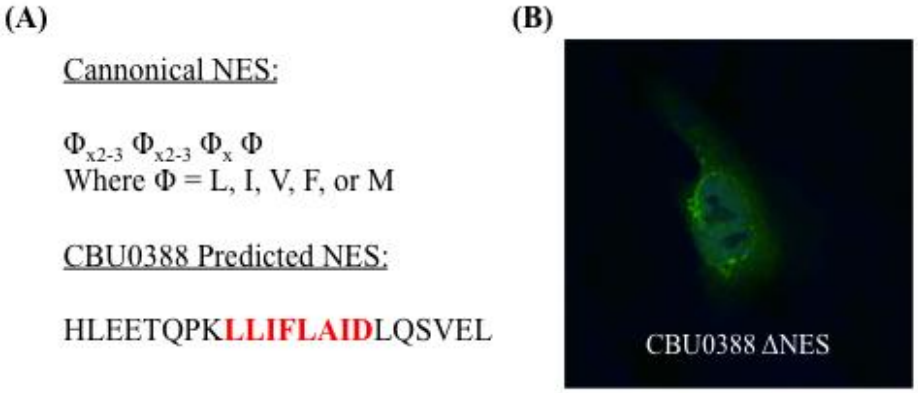

Figure 3.8. CBU0388 traffics out of the nucleus with a nuclear export signal. (A) Predicted nuclear export signal based compared to a canonical sequence. The portion in red indicates the amino acids that match the canonical NES sequence. (B) Representative confocal microscopy image of HeLa cells transfected with CBU0388 ΔNES mutant. Images were taken 12 hours post-transfection.

We also identified a nuclear export signal [80] in the sequence for CBU0388 (Figure 3.8A). Nuclear export signals are usually a stretch of 4-5 hydrophobic amino acids, usually leucine, arranged with spacers so they can be recognized by the nuclear export receptor Crm1 [81]. The consensus sequence for a typical NES is shown in Figure 3.8A. To test the functionality of these sequences in CBU0388 trafficking, we transfected a deletion mutant lacking the NES. (Figure 3.8B). In the case of the NES

mutant, the protein can enter the nucleus through its NLS, but is unable to be recognized by the export receptor Crm1, and is trapped within the nucleus. These results were also confirmed using pharmacological inhibitor Leptomycin B (LepB), which inhibits Crm1-specific nuclear export [82]. Leptomycin B has been used for over 20 years and covalently binds specifically to the Cysteine-529 residue of Crm1 [83]. The high specificity of LepB eliminates the possibility of treatment interfering with another molecule causing an artifactual result.

CBU0388's transfection-associated toxicity is dependent on nuclear trafficking. Similar to the toxicity seen when CBU0388 is expressed in yeast [84], transient transfection in mammalian cells also resulted in toxicity. This phenotype has made exploring functionality in these conditions very limited. To understand more about this cellular death phenotype, we investigated the type of cell death these cells undergo. As shown in Figure 3.9, this toxicity is a result of apoptotic cell death, as determined by measuring caspase 3/7 activiation during expression in HeLa cells. At eight hours post transfection when no GFP-tagged protein is produced, the caspase activity of both the vector and CBU0388 are similar. After twenty-four hours, however, there is a marked increase in the amount of caspase activation in the cells transfected with CBU0388. The cellular death induced by expression of CBU0388 is similar to treatment with the potent apoptosis inducer Staurosporine. Although the activation of Caspase 3/7 is not the only indicator of apoptotic death, it was the one we used. Using other readouts for apoptosis could further add to the mechanism of this toxicity. Since *C. burnetii* does not cause

apoptotic cell death [58] it can be almost certain that the toxic result is simply an artifact of over-expressing CBU0388 in these cells.

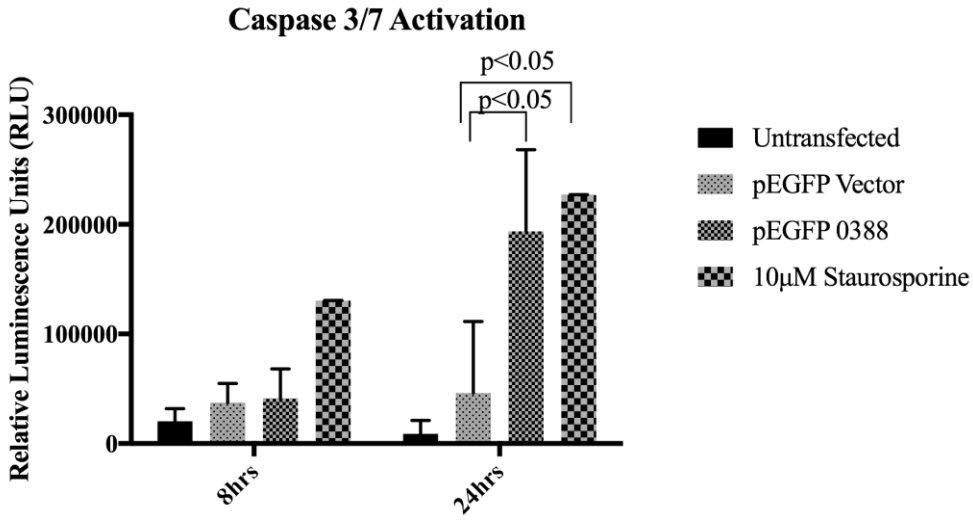

Figure 3.9 Transfection of CBU0388 causes apoptotic cell death. HeLa cells were transfected with indicated plasmids or subjected to Staurosporine treatment and analyzed for apoptosis with the Promega ApoTox-Glo^{TM} Triplex Assay kit, according to manufacturer's protocol. Graph shows levels of apoptotic cells after eight or twenty-four hours post transfection.

This cellular toxicity was alleviated, however, when CBU0388 was expressed without the NLS or treatment with the pharmacological inhibitor Importazole, which prevents binding of the cargo protein to Importin B (Figure 3.10A).

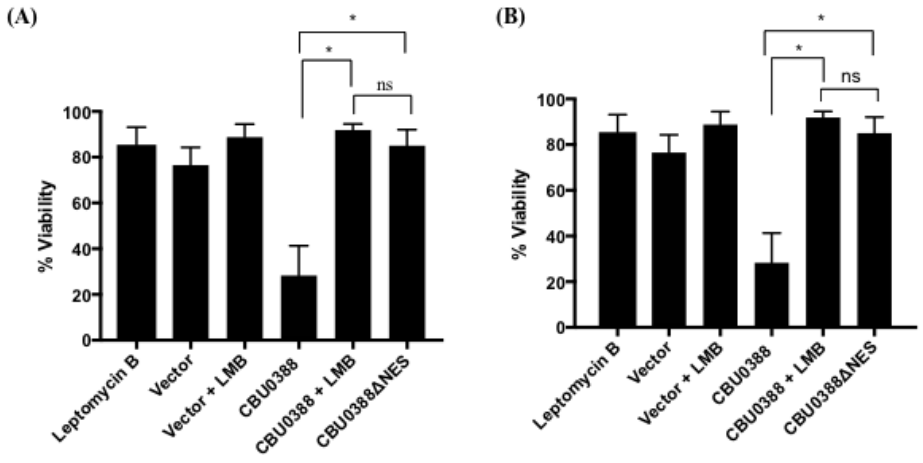

Figure 3.10. **Toxicity of CBU0388 is dependent on its ability to complete a nuclear import-export cycle.** (A) HeLa cells were transfected with EGFP N-terminally tagged CBU0388, CBU0388 ΔNES, CBU0388 ΔNLS, or vector alone. Cells were treated with Importazole for 1 hour before Trypan Blue staining for viability was tested. (B) HeLa cells were transfected as in (A) but treated with Leptomycin B (LMB) for 4 hours before Trypan blue was measured. *$p<0.05$

Conversely, deleting the NES or inhibiting the nuclear export receptor Crm1, prevents the toxicity seen with the full-length CBU0388 (Figure 3.10B). Expressing CBU0388 defective in entering or leaving the nucleus, respectively, does not cause toxicity. Therefore, a complete nuclear trafficking appears to be required for full functionality and the resulting cellular toxicity.

CBU0388 has structural similarity to the export receptor Crm1. We used the online protein structural analysis software Raptor X (http://raptorx.uchicago.edu/) to predict the structure of CBU0388. This predicted a folded protein with structural homology to Crm1, the primary nuclear export receptor.

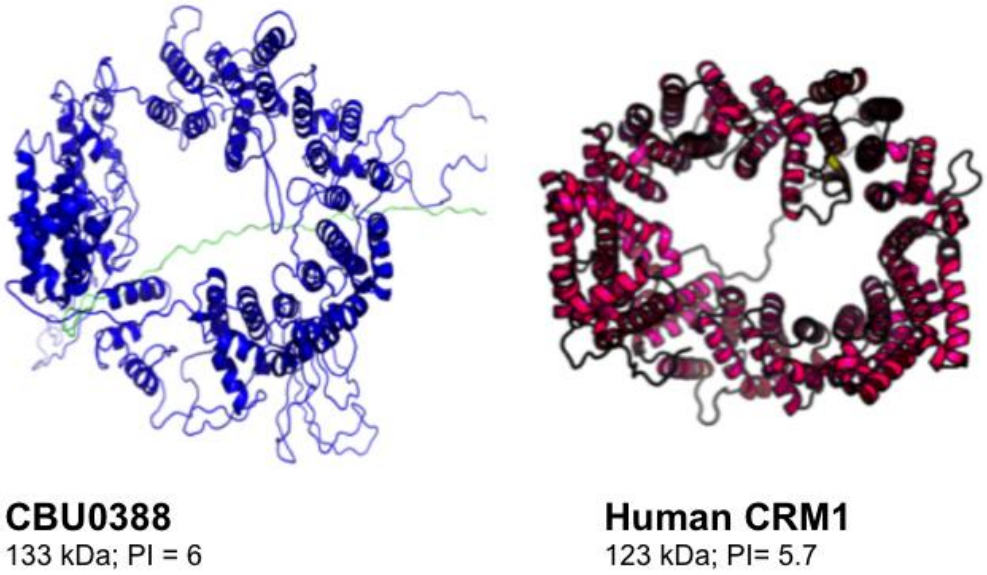

Figure 3.11. Structural comparison of the predicted folding of CBU0388 and the crystal structure of Crm1. The RaptorX derived protein prediction of CBU0388 (left) compared to the known crystal structure of Human CRM1. The structural similarity was statistically significant. p value = 2.26×10^{-6}.

Here, we present our working model of how the nuclear trafficking of CBU0388 occurs in a cell infected with *C. burnetii* (Figure 3.12). Once *C. burnetii* infects a host cell, it secretes CBU0388 into the cytoplasm. Once secreted, the protein then traffics into the nucleus via a canonical NLS. Unfortunately, at this point we still do not understand

the protein's nuclear function. CBU0388 is then exported out of the nucleus through interaction with its NES and the export receptor Crm1.

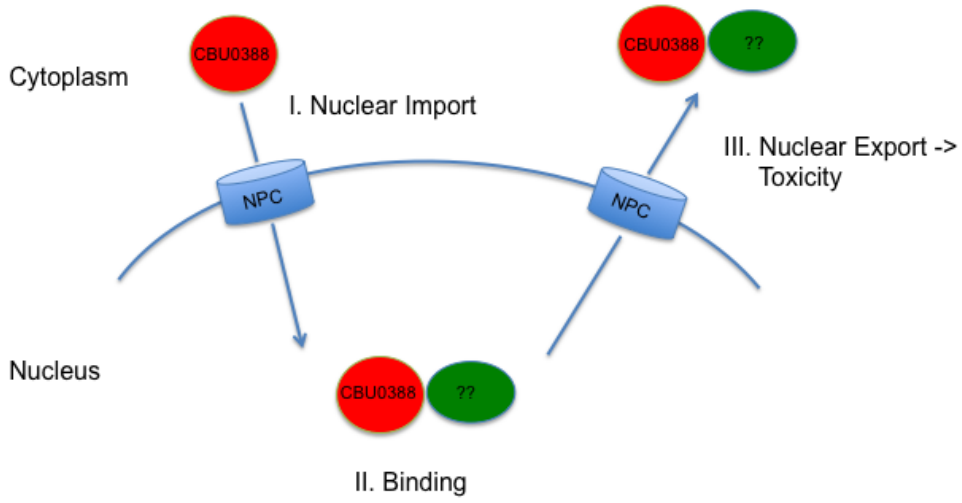

Figure 3.12. Working model of the trafficking of CBU0388 in host cells. Step I. Secreted CBU0388 is imported into the host nucleus through NLS. Step II. CBU0388 binds to an unknown factor, depicted as Protein X, in the nucleus. Step III. CBU0388 is exported along with Protein X resulting in mislocalization of Protein X which results in **Figure 3.12 cont.** toxicity during ectopic expression. Future studies will be to identify Protein X and the downstream results during infection. NPC = Nuclear pore complex.

EMAP analysis of CBU0388 reveals novel pathway targets. To further investigate the role of CBU0388 in the host cell, we employed the power of yeast genetics in Epistatic Mini-array Profile (EMAP) technology. This technique was developed originally to identify shared biological pathways between *Saccharomyces cerevisiae* and *Schizosaccharomyces pombe* [85]. In a novel screen, EMAP technology was used to evaluate genetic interactions between *S. cerevisiae* mutants and effectors from across three different pathogens: *C. burnetii*, *Salmonella enterica* serovar Typhimurium, and *Brucella melitensis* [61]. Yeast expressing CBU0388 were crossed with a mutant library containing approximately 4600 single deletion mutants and effect on growth was scored in a semi-quantitative manner. The resulting data can be sorted into statistically significant measure of correlation, represented by a z-score. The results correlate strongly with genes involved in spindle pole body positioning, kinetochore, and segregation of chromosomes, consistent with a potential modulation of nuclear division and the cell cycle. The gene ontology (GO) terms with the highest correlation with expression of CBU0388 indicate a potential effect on host cell cycle and division (Figure 3.13).

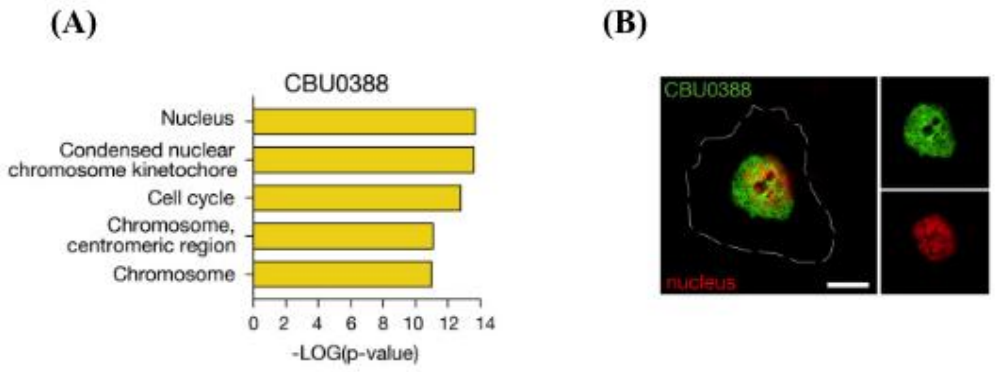

Figure 3.13. Gene Ontology terms predicted by the EMAP Screen. (A) Enriched GO terms for significantly correlating genetic interaction profiles for CBU0388. (B) HeLa cells transiently transfected to express GFP-CBU0388, co-stained with Hoechst to visualize nuclei. Scale bar, 10μm. **Figure adapted from Patrick and Wojcechowskyj, *et al.* (2018). *Cell Systems [61].***

***C. burnetii* does not appear to manipulate cell cycle of the host cell.** The EMAP results that point to cell cycle manipulation was particularly interesting. *C. burnetii* establishes a long term, sometimes persistently infected cell population. Therefore, it would be interesting to see if there was manipulation of the host cell cycle. Early experiments looking at cell DNA content as a measure of cell cycle stage have shown

that *C. burnetii* does not cause an interruption in cell cycle [86]. That same study also shows that while cell division occurs normally, the CCV is not divided at all. Only one of the resulting daughter cells remains infected, while the other becomes uninfected. No other studies have been done to test further manipulation of host cell cycle. It could be likely that while the global cell cycle stages occur normally, there is a subtle change induced by *C. burnetii*. This, of course, is harder to detect without knowing what specific aspects to check. We wanted to see if we could replicate these past cell cycle results. We assayed a number of infected cell types (J774A.1, L929 and HeLa cells) with similar results across experiments. The flow cytometry graphs (Figure 3.14) show similar DNA profiles across all infected conditions, which recapitulate the historical data.

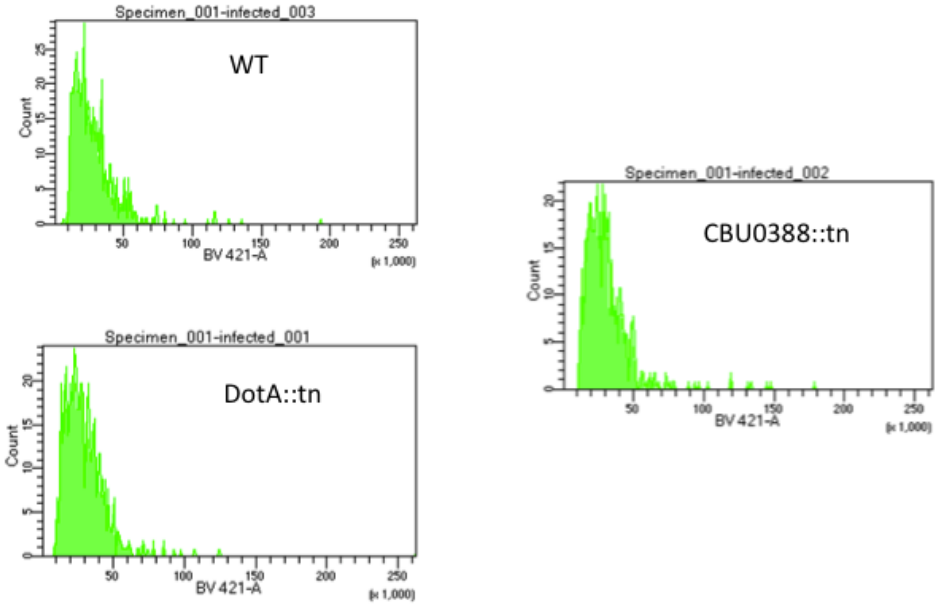

Figure 3.14. *C. burnetii* does not appear to manipulate cell cycle progression. Infected L929 cells were stained and subjected to flow cytometry analysis to assess DNA content in the infected cells. The figure above shows one representative experiment.

Serum starvation synchronization temporarily prevents toxicity induced by expression of CBU0388. In order to try to assess the correlation between expression of CBU0388 and cell cycle, we decided to synchronize the cells before transfection. While this was originally meant to be a tool, the experimental results were unexpected. Serum starvation caused all the cells to stall at the G_1 phase of mitosis [87]. This treatment, of course, has other pleotropic effects. One notable change is that serum starvation changes

the transcriptional profile of the cell [88]. When we serum starved the cells before transfection, we no longer saw CBU0388-dependent cellular death (Figure 3.15). While previous experiments showed almost no cellular viability after only twelve hours of transfection, serum starved cells still had normal viability after twenty-four hours.

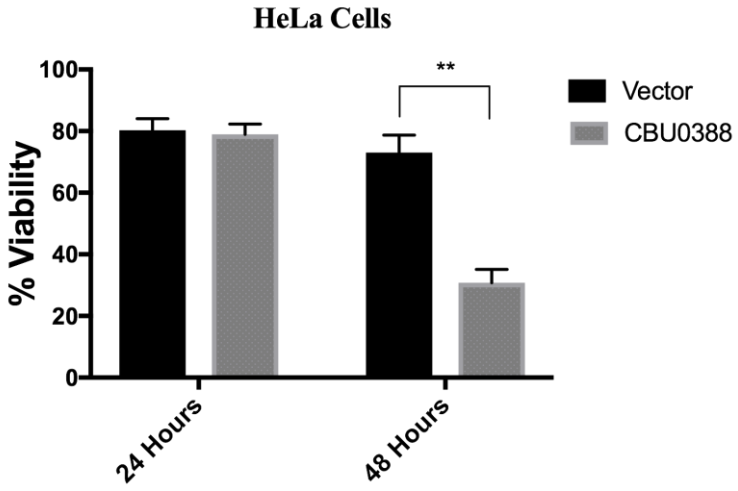

Figure 3.15 Serum starvation prevents CBU0388 toxicity in transient transfection. HeLa cells were serum starved to synchronize them at G_1 phase twelve hours before transient transfection. Serum was added back at time of transfection to restart cell cycle. Trypan blue staining was done at twenty-four hours and fourty-eight hours post transfection. ** $p<0.005$

The addition of serum at the time of transfection would restart normal cell cycle, allowing for normal transcriptional and protein synthesis activity to begin again. The synchronized cells were able to express a nuclear-localized CBU0388 without causing the typically seen toxicity. Prolonged expression under normal cell cycle caused the toxicity to return, however, after forty-eight hours.

Discussion

While several nuclear localized *C. burnetii* T4SS effectors have been identified, CBU0388 is the first to be characterized for its role in pathogenesis. This is also the first instance where action in the nucleus of the cell can be connected to biogenesis of the pathogen-containing vacuole.

Nucleomodulins and cylomodulins are a broad class of virulence factors that can act in the nucleus of the host. While it has not be determined if *C. burnetii* manipulates the mitotic cell cycle during infection, three effectors appear to inhibit exogenously stimulated apoptosis to enable host survival and CCV development [57, 89]. Therefore, the prediction from the EMAP screen that CBU0388 may act as a nucleocyclin is innovative, and if confirmed, could represent a novel mechanism for a secreted nuclear effector.

The biggest shortcoming of this research is the absence of complementation of the CBU0388::tn mutant. Major factors including size exclusion and plasmid availability complicated the complementation process. Despite multiple efforts, complementation attempts failed. In prior work, our laboratory was able to successfully complement a

mutation in a different gene in *trans* [31], but this did not fully work with CBU0388 (Figure 3.5). This method of complementation depends on cells that are doubly infected with both the WT and CBU0388::tn mutant strains at the same time. This is a rare event on its own, particularly over a long period of infection. The typical infection rate after a week is only about ten percent. This is also a result of cellular growth and only a fraction of cell remaining infected. While growth of the mutant could be seen by confocal microscopy in rare events by this method (data not shown), there was no significant change in the overall population that could be shown by qPCR.

The only other time our lab has made a successful complementation was with a large (10 kbp) vector expressing the protein in the mutant strain [59]. This was still only partially effective to restore the growth of the mutant in this case. With the size of the vector, we were not able to use this with the large CBU0388 protein. We tried using other vector plasmids to deliver the CBU0388 protein into the CBU0388::tn mutant without success. We did have the entire genome of the CBU0388::tn mutant sequenced (data not shown) which confirmed the transposon insertion in the single CBU0388 ORF. Therefore lack of complementation is not due to multiple mutations or mixed culture.

The latest strategy for complementation tried was using a Tn7 Tet^R-inducible plasmid containing a 3XHA-tagged CBU0388. This vector plasmid was previously used for complementation in a *C. burnetii* mutant and showed a rescue of growth [90]. We were able to show induction of the CBU0388 protein in ACCM-2 grown bacterial cells (Appendix C) but the kinetics of protein expression in intracellular infection became more difficult. We did not see a rescue of growth in any of the induction conditions we

tried, but protein kinetics could be to blame. Future studies will need to be done to either optimize this or create a new complementation strategy.

Another avenue that still needs to be explored in the mode of action of CBU0388. It could be argued that CBU0388 must be important for *C. burnetii* to continually express it as well as maintain such a large ORF in its genome. While the EMAP studies point to a possible role in cell cycle, no further experiments have been able to confirm this. Protein interaction studies have been difficult with the toxicity that comes with CBU0388 expression. We tried a pulldown and mass spectrometry with the CBU0388ΔNES and CBU0388ΔNLS mutants expressed in HEK293T cells, but it did not result in identification of any interaction partners. There was an overabundance of protein interactions, none of which had a high enough mass spectrometry score to merit follow-up analysis. One hypothesis could be that CBU0388 does actually interact with multiple proteins in the same way as Crm1 binds multiple cargo proteins, but most likely our results were due to high background with not enough expression of our tested proteins. The experiment should be repeated for better success.

CHAPTER IV

CONCLUSION

As an obligate intracellular pathogen, *C. burnetii* must possess multiple mechanisms to manipulate the host cell for its own benefit. The host cell nucleus is an obvious target for manipulation given its pivotal role as the site of such important cellular events such as transcription, DNA replication, and cell cycle. From the six potential type IV secretion-dependent nucleomodulin candidates (Table 4.1), this research explored the role of CBU0794 (Cig20) and CBU0388. This project resulted in discovery of a novel protein interaction between CBU0794 and the transcriptional activator protein TBL1XR1. Although the consequences of this interaction have not yet been elucidated, the pivotal role TBL1XR1 plays in multiple pathways could lead to very interesting transcriptional consequences. In addition, this project characterized CBU0388 as the first nuclear-localized effector in *C. burnetii* to play a role in pathogenesis. This protein, while made a challenge by its size and cellular toxicity, has been shown to potentially play an important role in cellular cycle manipulation during infection. A model of the role of both of these effectors in *C. burnetii* infection is presented below (Figure 4.1).

CBU Designation	Molecular Weight	Ectopic Expression Localization
CBU0129	14.1 kDa	Nuclear and Perinuclear (punctate)
CBU0388	161 kDa	Nuclear; Cytotoxic
CBU0393	20 kDa	Nuclear
CBU0794/Cig20	53.1 kDa	Nuclear
CBU1314	23.5 kDa	Nuclear
CBU1524/CaeA	25.1 kDa	Nuclear

Table 4.1. List of nuclear localized substrates in *C. burnetii.*

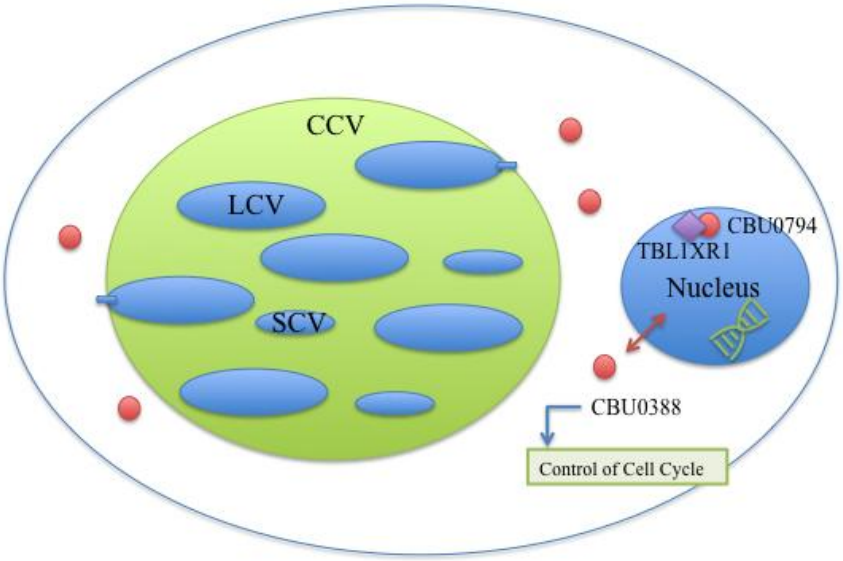

Figure 4.1. Final representative model of nucleomodulin action in *C. burnetii* infection. Infected cell depicting the large cell variant (LCV) and the small cell variant (SCV) of *C. burnetii* with an active type IV secretion system. In this case, CBU0794 and CBU0388 target the host nucleus in order to perform differential roles in transcriptional control and potential cell cycle modulation.

CBU0794

The result that CBU0794 bound to the protein TBL1XR1 brought a plethora of potential theories about the consequences of this interaction. The initial idea was that

CBU0794 bound to TBL1XR1 in order to prevent binding of the SMRT/NCoR to DNA, thus allowing transcription to occur. This was shown not to be the case, as the RNA-seq failed to show any activation of transcription in the presence of CBU0794 (Figure 2.10). It makes sense that *C. burnetii* would not want to activate overall cellular transcription in such a non-specific way. Since CBU0794 is present throughout infection, this must also be a long-term transcriptional modulation. Instead, some sort of controlled differential transcription would be more beneficial to the bacteria. Alternately, an upstream signal may have been necessary to cause the transcriptional response to be present.

Another hypothesis could be that CBU0794 was binding TBL1XR1 to cause degradation of the protein or the complex. This could be through some post-translational modification that would mark it for degradation. This also seemed to be ruled out as a hypothesis since protein levels of TBL1XR1 as well as SMRT and NCoR all appear to be the same both in the presence or absence of CBU0794 (Figure 2.8). Similarly, if CBU0794 were just sequestering TBL1XR1 from the SMRT/NCoR complex, the cell could compensate by increasing protein levels of TBL1XR1. This does not happen. You would also potentially see increased transcription in the case, but we fail to see that.

Another major hypothesis to consider is the involvement of CBU0794 in the Wnt/β-catenin pathway. In normal cells, the presence of the signaling molecule β-catenin causes TBL1XR1 to become SUMOylated, causing it to leave the SMRT/NCoR and form a new complex with β-catenin that directs transcription of Wnt-regulated genes. The presence of a higher molecular weight subspecies of TBL1XR1 in the presence of CBU0794 seems to support this theory (Figure 2.9). Of course, further confirmation of

this still needs to be done to determine if this is indeed a result of SUMOylation or some other post-translational modification such as phosporylation or ubiquitination.

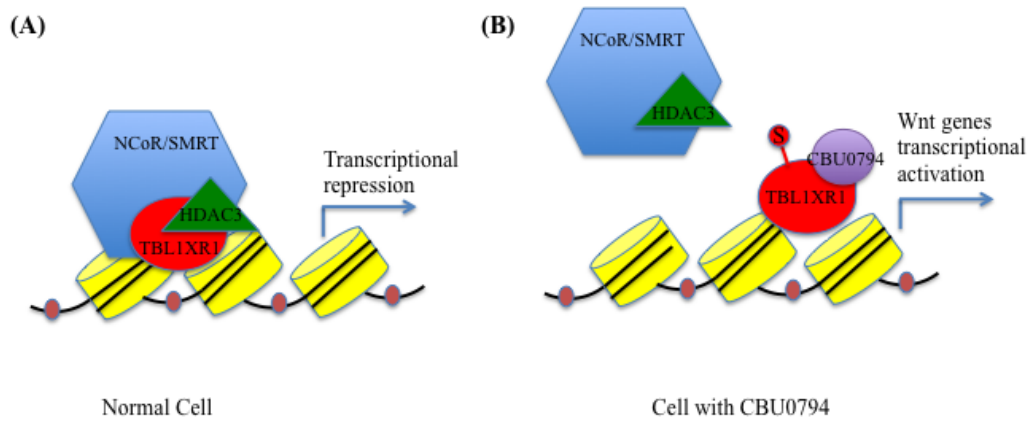

Figure 4.2. Hypothetical representation of the effect CBU0794 expression in the host cell. (A) An image representative of a normal cell with TBL1XR1 bound to the NCoR/SMRT complex as a transcriptional repressor. (B) Our hypothesis depicting **Figure 4.2 cont.** CBU0794 bound to a SUMOylated TBL1XR1, which redirects it from the NCoR/SMRT complex to be used to activate Wnt-regulated transcriptional activation.

In the CBU0794 pulldown, we only found TBL1XR1 alone, not other members of the SMRT/NCoR-HDAC3 complex. It would be safe to say then that CBU0794 interacts with TBL1XR1 alone, not in the context of a larger protein complex. Of course, the complex may not have been pulled down in the experiment due to the large size of the complex, protein degradation, or protein instability. A representation of our hypothesis of CBY0794 action is presented in Figure 4.2.

The obvious caveat to all of this data is that it was not done in the context of an infected cell. We do not have the ability to create a CBU0794 mutant in the context of this project. The addition of a deletion mutant of this protein in the future will provide further evidence of the important role of CBU0794 in *C. burnetii* pathogenesis. Another important experiment would be to confirm localization of CBU0794 to the nucleus during infection. This has proven to be a tricky experiment but could lend more information about the temporal and spatial requirements for CBU0794 during infection. This experiment could be done by microscopy or western blot using a tagged version of CBU0794 in *C. burnetii*.

CBU0388

CBU0388 has been a challenge to understand. Its remarkable size of a 161kDa protein makes it the largest effector protein in *C. burnetii*. In fact, its size is even more significant if you consider that *C. burnetii* has a relatively small genome in total. The coding region of CBU0388 takes up 0.2% of genetic coding space in the genome.

Despite evolutionary pressure over time, *C. burnetii* has retained this large protein as a secreted effector in acute isolates, so it can be inferred that it must be required.

We explored the requirement of this protein in a virulent SCID mouse model and multiple tissue culture cell lines. While complementation has been elusive, I have no doubt that the mutant phenotype is solely a result of the loss of CBU0388 during infection. The CBU0388::tn mutant was unable to grow in any cell line, whether an epithelial cell, macrophage cell line or primary macrophage. *C. burnetii* needs CBU0388 in a fundamental way, not specific to immune evasion or cell-specific recognition.

An interesting finding was the identification of functional nuclear trafficking domains that CBU0388 uses to both enter and leave the nucleus of the host cell. This in and out style nuclear trafficking is unique to this effector. While nuclear localization signals are common among nuclear effectors in bacteria, a nuclear export signal is not, although multiple reports of nucleocytoplasmic trafficking by viral proteins have been documented [91]. *C. burnetii* has evolved a unique effector protein that traffics similar to a eukaryotic protein. In fact, it seems to have more in common with a eukaryotic protein than a bacterial effector. My initial hypothesis was that CBU0388 was entering the nucleus to find a binding partner, termed Protein X. Once bound to its target, it could potentially mis-localize this Protein X into the cytoplasm so that the function of Protein X cannot be performed. In pulldown experiments, however, Protein X was unable to be identified using GFP-tagged NLS and NES mutants. This lack of result could be due to the methodology and transfection not being sufficient for detection by pulldown. It could also be that my hypothesis about Protein X was not correct.

Another hypothesis is that CBU0388 may not bind Protein X, but rather modify it in some way to prevent or enhance functionality. Assuming the identity of Protein X belongs to a protein important for allowing *C. burnetii* to grow in any cell type, it would be important to modulate its function for the benefit of the bacteria. This could be accomplished by activating Protein X through some modification such as phosphorylation or acetylation. Instead, CBU0388 could recruit E3 ligases to ubiquitinate Protein X for destruction but it does not contain any ligase domains. This hypothesis wouldn't explain the movement out of the nucleus, however, as this modification could easily occur in the nucleus.

Alternatively, CBU0388's nuclear movement may not result in a particular protein binding. That being, it may bind a whole host of proteins. Given its structural homology to the nuclear export receptor Crm1, it may be acting as a mimic to co-opt all nuclear export. In this case, CBU0388 could act as a shuttling protein to remove multiple components from the nucleus. This could be a way for *C. burnetii* to deliver nuclear components directly to the cytoplasm or CCV. Since we don't know most of the requirements for a stable CCV, it would be hard to determine if this was the case. We do not actually know if CBU0388 accumulates in the cytoplasm of an infected cell or if it interacts directly with the CCV. Localization of CBU0388 in an infected cell would answer this question. This hypothesis of CBU0388 acting as a bacterial-specific shuttle would most likely negate any specificity CBU0388 may have in its nuclear interactions.

Likely, one or more of these hypotheses could be true. Given its large size, CBU0388 may perform multiple actions during infection, including acting as a nuclear

shuttle. We can ask ourselves: what nuclear proteins would be worth employing such an effector as CBU0388 to modulate? The answer is not a simple one. Nor is it an obvious one.

Our EMAP yeast screen pointed towards a potential role of CBU0388 in cell cycle control. Despite my results and long-standing consensus that *C. burnetii* does not disrupt cell cycle, this does not rule out this hypothesis. Besides overt disruption of cell cycle, CBU0388 could play a role in modulating a key regulator for another purpose. The EMAP screen presents a profile matching profiles of yeast that express your effector protein with a profile of yeast genetic mutant. CBU0388 had the strongest data of all the effectors we tested, matching it to the nuclear division or cell cycle pathways. The fact that *C. burnetii* does not effect cell cycle provides further information to this finding and could point to a role in cellular division.

A unique feature of *C. burnetii* is that during cellular division, the CCV only goes to one single daughter cell instead of also splitting into two. After mitosis occurs, only one of the two resulting daughter cells stays infected while the other is uninfected [86]. This seems like a weird phenomenon if the bacteria want to maintain a persistently infected cell population. It could simply be a way to maintain its stealth pathogen status. Since we do not know how *C. burnetii* escapes a cell and spreads to others, answering these questions become difficult. One confounding factor is the requirement for CBU0388 in order to establish a replicative niche. There is no known data about the requirements for *C. burnetii* making a functional CCV. It's unclear what host nuclear factors could be crucial to establishing a CCV and initiating bacterial replication.

This is really the first step to understanding the role of CBU0388 in *C. burnetii.* We really don't know the consequences of CBU0388 action during infection, despite a clue that it is involved in chromatin segregation and division. Further studies should focus on establishing the precise protein interactions of CBU0388. Does it interact with a single protein partner or multiple? Does it bind DNA or RNA? Why does *C. burnetii* need such a large effector protein to traffic in and out of the nucleus?

Final Conclusions

Coxiella burnetii is an obligate intracellular pathogen that has developed a unique repertoire of type IV secreted effectors to promote its survival, vacuole formation, and intracellular replication. Over 100 secreted effectors have been identified through several screens, most of which lack a defined function. Of these, six have been described as having nuclear localization during ectopic expression in tissue culture cells. Two of these effectors, CBU0794 and CBU0388, have been highlighted in this study.

The nucleus has long been perceived as the brain of the cell, giving instructions for multiple cellular processes for the benefit of the cell. Modern research has further focused on the importance of bacterial manipulation of the nucleus to also allow bacteria to benefit. Bacteria have employed a class of secreted effectors, termed Nucelomodulins, to carry out targeted roles in manipulating the brain of the cell for survival of bacteria within host cells. While intracellular dynamics are complex, relying on multiple coordinating pathways, bacteria have evolved multiple strategies to co-opt these pathways. The effectors described here are only the first step in understanding the action

of nucleomodulins in *C. burnetii.* Future studies could reveal just how powerful and far-reaching is *C. burnetii*'s control of its host cell nucleus.

REFERENCES

1. van Schaik EJ, Chen C, Mertens K, Weber MM, Samuel JE. Molecular pathogenesis of the obligate intracellular bacterium Coxiella burnetii. *Nat Rev Microbiol. 2013;11*(8):561-73. doi: 10.1038/nrmicro3049. PubMed PMID: 23797173; PubMed Central PMCID: PMCPMC4134018.

2. Madariaga MG, Rezai K, Trenholme GM, Weinstein RA. Q fever: a biological weapon in your backyard. *The Lancet Infectious Diseases. 2003;3*(11):709-21. doi: 10.1016/s1473-3099(03)00804-1.

3. Roest HI, Tilburg JJ, van der Hoek W, Vellema P, van Zijderveld FG, Klaassen CH, et al. The Q fever epidemic in The Netherlands: history, onset, response and reflection. *Epidemiol Infect. 2011;139*(1):1-12. doi: 10.1017/S0950268810002268. PubMed PMID: 20920383.

4. Derrick EH. "Q" fever, a new fever entity: clinical features, diagnosis, and laboratory investigation. *Medical Journal of Australia. 1937;2*:281-99.

5. Eldin C, Melenotte C, Mediannikov O, Ghigo E, Million M, Edouard S, et al. From Q Fever to Coxiella burnetii Infection: a Paradigm Change. *Clinical microbiology reviews*. 2017;*30*(1):115-90. doi: 10.1128/CMR.00045-16. PubMed PMID: 27856520; PubMed Central PMCID: PMCPMC5217791.

6. Zhang G, Samuel JE. Vaccines against Coxiella infection. *Expert Rev Vaccines.* 2004;*3*(5):577-84. PubMed PMID: 15485337.

7. Hackstadt T, Peacock MG, Hitchcock PJ, Cole RL. Lipopolysaccharide variation in *Coxiella burnetii*: interstrain heterogeneity in structure and antigenicity. *Infection and immunity*. 1985;*48*(2):359-65.

8. Narasaki CT TR. Lipopolysaccharide of Coxiella burnetii. *Adv Exp Med Biol.* 2012;(948):65-90.

9. Moos A, Hackstadt T. Comparative virulence of intra-and interstrain lipopolysaccharide variants of *Coxiella burnetii* in the guinea pig model. *Infection and immunity*. 1987;*55*(5):1144-50.

10. Howe D, Shannon JG, Winfree S, Dorward DW, Heinzen RA. *Coxiella burnetii* Phase I and II Variants Replicate with Similar Kinetics in Degradative

Phagolysosome-Like Compartments of Human Macrophages. *Infection and immunity*. 2010;*78*(8):3465-74

11. Howe D, Mallavia LP. *Coxiella burnetii* exhibits morphological change and delays phagolysosomal fusion after internalization by J774A.1 cells. *Infection and immunity*. 2000;*68*(7):3815-21. PubMed PMID: 10858189.

12. Cutler SJ, Bouzid M, Cutler RR. Q fever. *J Infect.* 2007;*54*(4):313-8. PubMed PMID: 17147957.

13. Baca OG, Klassen DA, Aragon AS. Entry of *Coxiella burnetii* into host cells. *Acta Virol.* 1993;*37*(2-3):143-55. PubMed PMID: 8105658.

14. Capo C, Lindberg FP, Meconi S, Zaffran Y, Tardei G, Brown EJ, et al. Subversion of monocyte functions by *Coxiella burnetii*: impairment of the cross-talk between alphavbeta3 integrin and CR3. *J Immunol.* 1999;*163*(11):6078-85. PubMed PMID: 10570297.

15. Meconi S, Jacomo V, Boquet P, Raoult D, Mege J-L, Capo C. *Coxiella burnetii* Induces Reorganization of the Actin Cytoskeleton in Human Monocytes. *Infection and immunity.* 1998;*66*(11):5527-33

16. Voth DE, Heinzen RA. Lounging in a lysosome: the intracellular lifestyle of Coxiella burnetii. *Cell Microbiol.* 2007;9(4):829-40. doi: 10.1111/j.1462-5822.2007.00901.x. PubMed PMID: 17381428.

17. Kinchen JM, Ravichandran KS. Phagosome maturation: going through the acid test. *Nat Rev Mol Cell Biol*. 2008;*9*(10):781-95

18. Criscitiello MF, Dickman MB, Samuel JE, de Figueiredo P. Tripping on acid: trans-kingdom perspectives on biological acids in immunity and pathogenesis. *PLoS Pathog*. 2013;*9*(7):e1003402. doi: 10.1371/journal.ppat.1003402. PubMed PMID: 23874196; PubMed Central PMCID: PMCPMC3715416.

19. Gomes MS, Paul, S., Moreira, A.L., Appelberg, R., Rabino- vitch, M., and Kaplan, G. Survival of Mycobacterium avium and Mycobacterium tuberculosis in acidified vacu- oles of murine macrophages. *Infection and immunity.* 1999;*67*:3199-206.

20. Andreoli WK, Taniwaki NN, Mortara RA. Survival of Trypanosoma cruzi metacyclic trypomastigotes within Coxiella burnetii vacuoles: differentiation and replication within an acidic milieu. *Microbes Infect*. 2006;*8*(1):172-82. PubMed PMID: 16182585.

21. Fernandes MC, L'Abbate C, Kindro Andreoli W, Mortara RA. Trypanosoma cruzi cell invasion and traffic: influence of Coxiella burnetii and pH in a comparative study between distinct infective forms. *Microb Pathog*. 2007;*43*(1):22-36. PubMed PMID: 17448629.

22. Veras PST, de Chastellier C, Moreau M-F, Villiers V, Thibon M, Mattei D, et al. Fusion between large phagocytic vesicles: targeting of yeast and other particulates to phagolysosomes that shelter the bacterium *Coxiella burnetti* or the protozoan *Leishmania amazonensis* in Chinese hamster ovary cells. *Journal of Cell Science*. 1994;*107*:3065-76.

23. Drecktrah D, Knodler LA, Howe D, Steele-Mortimer O. Salmonella Trafficking is Defined by Continuous Dynamic Interactions with the Endolysosomal System. *Traffic.* 2007;*8*(3):212-25. doi: 10.1111/j.1600-0854.2006.00529.x.

24. Seshadri R, Paulsen IT, Eisen JA, Read TD, Nelson KE, Nelson WC, et al. Complete genome sequence of the Q-fever pathogen *Coxiella burnetii*. *Proceedings of the National Academy of Sciences of the United States of America.* 2003;*100*(9):5455-60. Epub 2003/04/22. PubMed PMID: 12704232; PubMed Central PMCID: PMC154366.

25. Segal G, Shuman HA. Possible origin of the *Legionella pneumophila* virulence genes and their relation to *Coxiella burnetii*. *Molecular microbiology.* 1999;*33*:667-8.

26. Zamboni DS, McGrath S, Rabinovitch M, Roy CR. *Coxiella burnetii* express type IV secretion system proteins that function similarly to components of the *Legionella pneumophila* Dot/Icm system. *Molecular microbiology*. 2003;*49*(4):965-76.

27. Zusman T, Yerushalmi G, Segal G. Functional similarities between the icm/dot pathogenesis systems of *Coxiella burnetii* and *Legionella pneumophila*. *Infection and immunity*. 2003;*71*(7):3714-23. Epub 2003/06/24. PubMed PMID: 12819052; PubMed Central PMCID: PMC161977.

28. Beare PA, Gilk SD, Larson CL, Hill J, Stead CM, Omsland A, et al. Dot/Icm type IVB secretion system requirements for Coxiella burnetii growth in human macrophages. *mBio*. 2011;*2*(4):e00175-11. Epub 2011/08/25. doi: 10.1128/mBio.00175-11. PubMed PMID: 21862628; PubMed Central PMCID: PMC3163939.

29. Carey KL, Newton HJ, Luhrmann A, Roy CR. The *Coxiella burnetii* Dot/Icm System Delivers a Unique Repertoire of Type IV Effectors into Host Cells and Is

Required for Intracellular Replication. *PLoS pathogens.* 2011;*7*(5):e1002056. Epub 2011/06/04. PubMed PMID: 21637816; PubMed Central PMCID: PMC3102713.

30. Chen C, Banga S, Mertens K, Weber MM, Gorbaslieva I, Tan Y, et al. Large-scale identification and translocation of type IV secretion substrates by *Coxiella burnetii*. *Proceedings of the National Academy of Sciences of the United States of America.* 2010. Epub 2010/11/26. PubMed PMID: 21098666; PubMed Central PMCID: PMC3003115.

31. Weber MM, Chen C, Rowin K, Mertens K, Galvan G, Zhi H, et al. Identification of Coxiella burnetii type IV secretion substrates required for intracellular replication and Coxiella-containing vacuole formation. *Journal of bacteriology.* 2013;*195*(17):3914-24. Epub 2013/07/03. doi: 10.1128/JB.00071-13. PubMed PMID: 23813730; PubMed Central PMCID: PMC3754607.

32. Voth DE, Beare PA, Howe D, Sharma UM, Samoilis G, Cockrell DC, et al. The Coxiella burnetii cryptic plasmid is enriched in genes encoding type IV secretion system substrates. *Journal of bacteriology*. 2011;*193*(7):1493-503. Epub 2011/01/11. doi: 10.1128/JB.01359-10. PubMed PMID: 21216993; PubMed Central PMCID: PMC3067651.

33. Voth DE, Howe D, Beare PA, Vogel JP, Unsworth N, Samuel JE, et al. The Coxiella burnetii ankyrin repeat domain-containing protein family is heterogeneous, with C-terminal truncations that influence Dot/Icm-mediated secretion. *Journal of bacteriology.* 2009;*191*(13):4232-42. Epub 2009/05/05. doi: 10.1128/JB.01656-08. PubMed PMID: 19411324; PubMed Central PMCID: PMC2698476.

34. van Schaik EJ, Case ED, Martinez E, Bonazzi M, Samuel JE. The SCID Mouse Model for Identifying Virulence Determinants in Coxiella burnetii. *Front Cell Infect Microbiol.* 2017;*7*:25. doi: 10.3389/fcimb.2017.00025. PubMed PMID: 28217558; PubMed Central PMCID: PMCPMC5289997.

35. Norville IH, Hartley MG, Martinez E, Cantet F, Bonazzi M, Atkins TP. Galleria mellonella as an alternative model of Coxiella burnetii infection. *Microbiology*. 2014;*160*(Pt 6):1175-81. doi: 10.1099/mic.0.077230-0. PubMed PMID: 24677067.

36. Davis BK, Wen H, Ting JP. The inflammasome NLRs in immunity, inflammation, and associated diseases. *Annu Rev Immunol.* 2011;*29*:707-35. doi: 10.1146/annurev-immunol-031210-101405. PubMed PMID: 21219188; PubMed Central PMCID: PMCPMC4067317.

37. Suhan ML, Shu-Yin C, Thompson HA. Transformation of *Coxiella burnetii* to ampicillin resistance. *Journal of bacteriology.* 1996;*178*:2701-8.

38. Beare PA, Larson CL, Gilk SD, Heinzen RA. Two systems for targeted gene deletion in Coxiella burnetii. *Appl Environ Microbiol.* 2012;*78*(13):4580-9. Epub 2012/04/24. doi: 10.1128/AEM.00881-12. PubMed PMID: 22522687; PubMed Central PMCID: PMC3370473.

39. Omsland A, Beare PA, Hill J, Cockrell DC, Howe D, Hansen B, et al. Isolation from Animal Tissue and Genetic Transformation of *Coxiella burnetii* Are Facilitated by an Improved Axenic Growth Medium. *Applied and environmental microbiology*. 2011;*77*(11):3720-5. Epub 2011/04/12. PubMed PMID: 21478315.

40. Omsland A, Cockrell DC, Howe D, Fischer ER, Virtaneva K, Sturdevant DE, et al. Host cell-free growth of the Q fever bacterium Coxiella burnetii. *Proceedings of the National Academy of Sciences of the United States of America.* 2009;*106*(11):4430-4. Epub 2009/02/28. doi: 10.1073/pnas.0812074106. PubMed PMID: 19246385; PubMed Central PMCID: PMC2657411.

41. Sandoz KM, Beare PA, Cockrell DC, Heinzen RA. Complementation of Arginine Auxotrophy for Genetic Transformation of Coxiella burnetii by Use of a Defined Axenic Medium. *Appl Environ Microbiol.* 2016;*82*(10):3042-51. doi: 10.1128/AEM.00261-16. PubMed PMID: 26969695; PubMed Central PMCID: PMCPMC4959063.

42. Beare PA, Sandoz KM, Larson CL, Howe D, Kronmiller B, Heinzen RA. Essential role for the response regulator PmrA in Coxiella burnetii type 4B secretion and colonization of mammalian host cells. *Journal of bacteriology.* 2014;*196*(11):1925-40. Epub 2014/03/13. doi: 10.1128/JB.01532-14. PubMed PMID: 24610709; PubMed Central PMCID: PMC4010987.

43. Newton HJ, Kohler LJ, McDonough JA, Temoche-Diaz M, Crabill E, Hartland EL, et al. A screen of Coxiella burnetii mutants reveals important roles for Dot/Icm effectors and host autophagy in vacuole biogenesis. *PLoS pathogens*. 2014;*10*(7):e1004286. Epub 2014/08/01. doi: 10.1371/journal.ppat.1004286. PubMed PMID: 25080348; PubMed Central PMCID: PMC4117601.

44. Latomanski EA, Newton P, Khoo CA, Newton HJ. The Effector Cig57 Hijacks FCHO-Mediated Vesicular Trafficking to Facilitate Intracellular Replication of Coxiella burnetii. *PLoS pathogens*. 2016;*12*(12):e1006101. doi: 10.1371/journal.ppat.1006101. PubMed PMID: 28002452; PubMed Central PMCID: PMCPMC5176192.

45. Larson CL1 ME, 3, Beare PA1, Jeffrey B4, Heinzen RA1, Bonazzi M2,3. Right on Q: genetics begin to unravel Coxiella burnetii host cell interactions. *Future Microbiol.* 2016 Jul;*11*:919-39.

46. Martinez E, Allombert J, Cantet F, Lakhani A, Yandrapalli N, Neyret A, et al. Coxiella burnetii effector CvpB modulates phosphoinositide metabolism for optimal vacuole development. *Proceedings of the National Academy of Sciences of the United States of America.* 2016;*113*(23):E3260-9. doi: 10.1073/pnas.1522811113. PubMed PMID: 27226300; PubMed Central PMCID: PMCPMC4988616.

47. Kohler LJ, Reed Sh C, Sarraf SA, Arteaga DD, Newton HJ, Roy CR. Effector Protein Cig2 Decreases Host Tolerance of Infection by Directing Constitutive Fusion of Autophagosomes with the Coxiella-Containing Vacuole. *mBio.* 2016;*7*(4). doi: 10.1128/mBio.01127-16. PubMed PMID: 27435465; PubMed Central PMCID: PMCPMC4958265.

48. Bierne H, Cossart P. When bacteria target the nucleus: the emerging family of nucleomodulins. *Cell Microbiol.* 2012;*14*(5):622-33. doi: 10.1111/j.1462-5822.2012.01758.x. PubMed PMID: 22289128.

49. Lebreton A, Lakisic G, Job V, Fritsch L, Tham TN, Camejo A, et al. A bacterial protein targets the BAHD1 chromatin complex to stimulate type III interferon response. *Science.* 2011;*331*(6022):1319-21. Epub 2011/01/22. doi: 10.1126/science.1200120. PubMed PMID: 21252314.

50. Kovarik P, Castiglia V, Ivin M, Ebner F. Type I Interferons in Bacterial Infections: A Balancing Act. *Front Immunol.* 2016;*7*:652. doi: 10.3389/fimmu.2016.00652. PubMed PMID: 28082986; PubMed Central PMCID: PMCPMC5183637.

51. Boxx Gayle M, Cheng G. The Roles of Type I Interferon in Bacterial Infection. *Cell host & microbe.* 2016;*19*(6):760-9. doi: 10.1016/j.chom.2016.05.016.

52. Nougayrede JP, Taieb F, De Rycke J, Oswald E. Cyclomodulins: bacterial effectors that modulate the eukaryotic cell cycle. *Trends Microbiol.* 2005;*13*(3):103-10. doi: 10.1016/j.tim.2005.01.002. PubMed PMID: 15737728.

53. Oswald E, Nougayrede JP, Taieb F, Sugai M. Bacterial toxins that modulate host cell-cycle progression. *Current opinion in microbiology.* 2005;*8*(1):83-91. doi: 10.1016/j.mib.2004.12.011. PubMed PMID: 15694861.

54. Marchès O, Ledger TN, Boury M, Ohara M, Tu X, Goffaux F, et al. Enteropathogenic and enterohaemorrhagic Escherichia coli deliver a novel effector

called Cif, which blocks cell cycle G2/M transition. *Molecular microbiology.* 2003;*50*(5):1553-67. doi: 10.1046/j.1365-2958.2003.03821.x.

55. Schafer W, Eckart RA, Schmid B, Cagkoylu H, Hof K, Muller YA, et al. Nuclear trafficking of the anti-apoptotic Coxiella burnetii effector protein AnkG requires binding to p32 and Importin-alpha1. *Cellular microbiology*. 2017;*19*(1). doi: 10.1111/cmi.12634. PubMed PMID: 27328359.

56. Weber MM, Faris R, McLachlan JT, Tellez A, Wright WU, Galvan G, et al. Modulation of the host transcriptome by Coxiella burnetii nuclear effector Cbu1314. *Microbes and Infection.* 2016;Volume *18*(Issue 5):336-45. doi: https://doi.org/10.1016/j.micinf.2016.01.003.

57. Klingenbeck L, Eckart RA, Berens C, Luhrmann A. The Coxiella burnetii type IV secretion system substrate CaeB inhibits intrinsic apoptosis at the mitochondrial level. *Cellular microbiology*. 2012. Epub 2012/11/07. doi: 10.1111/cmi.12066. PubMed PMID: 23126667.

58. Bisle S, Klingenbeck L, Borges V, Sobotta K, Schulze-Luehrmann J, Menge C, et al. The inhibition of the apoptosis pathway by the Coxiella burnetii effector protein CaeA requires the EK repetition motif, but is independent of survivin. Virulence. 2016;7(4):400-12. doi: 10.1080/21505594.2016.1139280. PubMed PMID: 26760129; PubMed Central PMCID: PMCPMC4871633.

59. Weber MM, Faris R, van Schaik EJ, McLachlan JT, Wright WU, Tellez A, et al. The Type IV Secretion System Effector Protein CirA Stimulates the GTPase Activity of RhoA and Is Required for Virulence in a Mouse Model of Coxiella burnetii Infection. *Infection and immunity.* 2016;*84*(9):2524-33. doi: 10.1128/IAI.01554-15. PubMed PMID: 27324482; PubMed Central PMCID: PMCPMC4995899.

60. Letunic I, Doerks T, Bork P. SMART: recent updates, new developments and status in 2015. *Nucleic Acids Res*. 2015;*43*(Database issue):D257-60. doi: 10.1093/nar/gku949. PubMed PMID: 25300481; PubMed Central PMCID: PMCPMC4384020.

61. Patrick KL, Wojcechowskyj JA, Bell SL, Riba MN, Jing T, Talmage S, et al. Quantitative Yeast Genetic Interaction Profiling of Bacterial Effector Proteins Uncovers a Role for the Human Retromer in Salmonella Infection. *Cell Syst.* 2018. doi: 10.1016/j.cels.2018.06.010. PubMed PMID: 30077634.

62. Sandoz KM, Popham DL, Beare PA, Sturdevant DE, Hansen B, Nair V, et al. Transcriptional Profiling of Coxiella burnetii Reveals Extensive Cell Wall Remodeling in the Small Cell Variant Developmental Form. *PloS one.*

2016;*11*(2):e0149957. doi: 10.1371/journal.pone.0149957. PubMed PMID: 26909555; PubMed Central PMCID: PMCPMC4766238.

63. Nguyen Ba AN, Pogoutse A, Provart N, Moses AM. NLStradamus: a simple Hidden Markov Model for nuclear localization signal prediction. *BMC Bioinformatics.* 2009;*10*:202. doi: 10.1186/1471-2105-10-202. PubMed PMID: 19563654; PubMed Central PMCID: PMCPMC2711084.

64. Kosugi S, Hasebe M, Tomita M, Yanagawa H. Systematic identification of cell cycle-dependent yeast nucleocytoplasmic shuttling proteins by prediction of composite motifs. *Proceedings of the National Academy of Sciences of the United States of America.* 2009;*106*(25):10171-6. doi: 10.1073/pnas.0900604106. PubMed PMID: 19520826; PubMed Central PMCID: PMCPMC2695404.

65. Mason JM, Arndt KM. Coiled coil domains: stability, specificity, and biological implications. *Chembiochem.* 2004;*5*(2):170-6. doi: 10.1002/cbic.200300781. PubMed PMID: 14760737.

66. Kruusvee V, Lyst MJ, Taylor C, Tarnauskaite Z, Bird AP, Cook AG. Structure of the MeCP2-TBLR1 complex reveals a molecular basis for Rett syndrome and related disorders. *Proceedings of the National Academy of Sciences of the United States of America.* 2017;*114*(16):E3243-E50. doi: 10.1073/pnas.1700731114. PubMed PMID: 28348241; PubMed Central PMCID: PMCPMC5402415.

67. Yoon HG CD, Huang ZQ, Li J, Fondell JD, Qin J, Wong J. Purification and functional characterization of the human N-CoR complex: the roles of HDAC3, TBL1 and TBLR1. *EMBO.* 2003;*22*(6):1336-46.

68. Perissi V AA, Glass CK, Rose DW, Rosenfeld MG. A Corepressor/Coactivator Exchange Complex Required for Transcriptional Activation by Nuclear Receptors and Other Regulated Transcription Factors. *Cell.* 2004;*116*:511-26.

69. Perissi V, Scafoglio, C., Zhang, J., Ohgi, K., Rose, DW.,, Glass C, and , Rosenfeld M. TBL1 and TBLR1 Phosphorylation on Regulated Gene Promoters Overcomes Dual CtBP and NCoR/SMRT Transcriptional Repression Checkpoints. *Molecular cell*. 2008;*29*(6):755-66.

70. Lee SK KJ, Lee YC, Cheong J, Lee JW. Silencing mediator of retinoic acid and thyroid hormone receptors, as a novel transcriptional corepressor molecule of activating protein-1, nuclear factor-kappaB, and serum response factor. *Journal of Biological Chemistry.* 2000;*275*(17):12470-4.

71. Li JY DG, Wang J, Zhang X. TBL1XR1 in physiological and pathological states. *Am J Clin Exp Urol.* 2015;*3*(1):13-23. PubMed Central PMCID: PMCPMC4446378.

72. Li J, Wang CY. TBL1-TBLR1 and beta-catenin recruit each other to Wnt target-gene promoter for transcription activation and oncogenesis. *Nat Cell Biol.* 2008;*10*(2):160-9. doi: 10.1038/ncb1684. PubMed PMID: 18193033.

73. Clevers H, Nusse R. Wnt/beta-catenin signaling and disease. *Cell*. 2012;*149*(6):1192-205. doi: 10.1016/j.cell.2012.05.012. PubMed PMID: 22682243.

74. Choi HK, Choi KC, Yoo JY, Song M, Ko SJ, Kim CH, et al. Reversible SUMOylation of TBL1-TBLR1 regulates beta-catenin-mediated Wnt signaling. *Molecular cell.* 2011;*43*(2):203-16. doi: 10.1016/j.molcel.2011.05.027. PubMed PMID: 21777810.

75. Lina TT, Luo T, Velayutham TS, Das S, McBride JW. Ehrlichia Activation of Wnt-PI3K-mTOR Signaling Inhibits Autolysosome Generation and Autophagic Destruction by the Mononuclear Phagocyte. *Infection and immunity*. 2017;*85*(12). doi: 10.1128/IAI.00690-17. PubMed PMID: 28993455; PubMed Central PMCID: PMCPMC5695117.

76. Brandenburg J, Reiling N. The Wnt Blows: On the Functional Role of Wnt Signaling in Mycobacterium tuberculosis Infection and Beyond. *Front Immunol.* 2016;*7*:635. doi: 10.3389/fimmu.2016.00635. PubMed PMID: 28082976; PubMed Central PMCID: PMCPMC5183615.

77. Chen C, Bouman TJ, Beare PA, Mertens K, Zhang GQ, Russell-Lodrigue KE, et al. A systematic approach to evaluate humoral and cellular immune responses to Coxiella burnetii immunoreactive antigens. *Clin Microbiol Infect.* 2009. Epub 2009/03/14. doi: CLM2206 [pii]10.1111/j.1469-0691.2008.02206.x. PubMed PMID: 19281461.

78. Stead CM, Omsland A, Beare PA, Sandoz KM, Heinzen RA. Sec-mediated secretion by Coxiella burnetii. *BMC Microbiol.* 2013;*13*:222. doi: 10.1186/1471-2180-13-222. PubMed PMID: 24093460; PubMed Central PMCID: PMCPMC3882888.

79. Zusman T, Aloni G, Halperin E, Kotzer H, Degtyar E, Feldman M, et al. The response regulator PmrA is a major regulator of the icm/dot type IV secretion system in Legionella pneumophila and Coxiella burnetii. *Molecular microbiology.* 2007;*63*(5):1508-23. Epub 2007/02/17. doi: 10.1111/j.1365-2958.2007.05604.x. PubMed PMID: 17302824.

80. la Cour T, Kiemer L, Molgaard A, Gupta R, Skriver K, Brunak S. Analysis and prediction of leucine-rich nuclear export signals. *Protein Eng Des Sel*. 2004;*17*(6):527-36. doi: 10.1093/protein/gzh062. PubMed PMID: 15314210.

81. Fung HY, Fu SC, Chook YM. Nuclear export receptor CRM1 recognizes diverse conformations in nuclear export signals. *Elife*. 2017;*6*. doi: 10.7554/eLife.23961. PubMed PMID: 28282025; PubMed Central PMCID: PMCPMC5358978.

82. Kudo N MN, Taoka H, Fujiwara D, Schreiner EP, Wolff B, Yoshida M, Horinouchi S. Leptomycin B inactivates CRM1/exportin 1 by covalent modification at a cysteine residue in the central conserved region. *Proceedings of the National Academy of Sciences of the United States of America.* 1999;*96*(16):9112-7. PubMed Central PMCID: PMCPMC17741.

83. Kudo N MN, Taoka H, Fujiwara D, Schreiner EP, Wolff B, Yoshida M, Horinouchi S. Leptomycin B inactivates CRM1/exportin 1 by covalent modification at a cysteine residue in the central conserved region. *Proc Natl Acad Sci U S A* 1999;*96*(16):9112-7. doi: https://doi.org/10.1073/pnas.96.16.9112. PubMed Central PMCID: PMCPMC17741.

84. Lifshitz Z, Burstein D, Schwartz K, Shuman HA, Pupko T, Segal G. Identification of novel Coxiella burnetii Icm/Dot effectors and genetic analysis of their involvement in modulating a mitogen-activated protein kinase pathway. *Infection and immunity.* 2014;*82*(9):3740-52. Epub 2014/06/25. doi: 10.1128/IAI.01729-14. PubMed PMID: 24958706; PubMed Central PMCID: PMC4187803.

85. Patrick KL, Ryan CJ, Xu J, Lipp JJ, Nissen KE, Roguev A, et al. Genetic interaction mapping reveals a role for the SWI/SNF nucleosome remodeler in spliceosome activation in fission yeast. *PLoS genetics.* 2015;*11*(3):e1005074. Epub 2015/04/01. doi: 10.1371/journal.pgen.1005074. PubMed PMID: 25825871; PubMed Central PMCID: PMC4380400.

86. Baca OG, Scott TO, Akporiaye ET, DeBlassie R, Crissman HA. Cell cycle distribution patterns and generation times of L929 fibroblast cells persistently infected with *Coxiella burnetii*. *Infection and immunity.* 1985;*47*(2):366-9. Epub 1985/02/01. PubMed PMID: 3967922.

87. Castellano E, Guerrero, C., Núñez,A. , De Las Rivas, J. and Santos, E. Serum-dependent transcriptional networks identify distinct functional roles for H-Ras and N-Ras during initial stages of the cell cycle. *Genome biology*. 2009;*10*. doi: 10.1186/gb-2009-10-11-r123).

88. Iyer VR1 EM, Ross DT, Schuler G, Moore T, Lee JC, Trent JM, Staudt LM, Hudson J Jr, Boguski MS, Lashkari D, Shalon D, Botstein D, Brown PO. The transcriptional program in the response of human fibroblasts to serum. *Science*. 1999;*283*(5398):83-7.

89. Eckart RA, Bisle S, Schulze-Luehrmann J, Wittmann I, Jantsch J, Schmid B, et al. Antiapoptotic activity of Coxiella burnetii effector protein AnkG is controlled by p32-dependent trafficking. *Infection and immunity.* 2014;*82*(7):2763-71. doi: 10.1128/IAI.01204-13. PubMed PMID: 24733095; PubMed Central PMCID: PMCPMC4097630.

90. Larson CL, Beare PA, Howe D, Heinzen RA. Coxiella burnetii effector protein subverts clathrin-mediated vesicular trafficking for pathogen vacuole biogenesis. *Proceedings of the National Academy of Sciences of the United States of America.* 2013;*110*(49):E4770-9. doi: 10.1073/pnas.1309195110. PubMed PMID: 24248335; PubMed Central PMCID: PMCPMC3856779.

91. Rivas S, Genin S. A plethora of virulence strategies hidden behind nuclear targeting of microbial effectors. *Front Plant Sci*. 2011;*2*:104. doi: 10.3389/fpls.2011.00104. PubMed PMID: 22639625; PubMed Central PMCID: PMCPMC3355726.

APPENDIX A

One way to understand the effect of CBU0794 on TBL1XR1 was to observe the transcriptional phenotype in an infection.

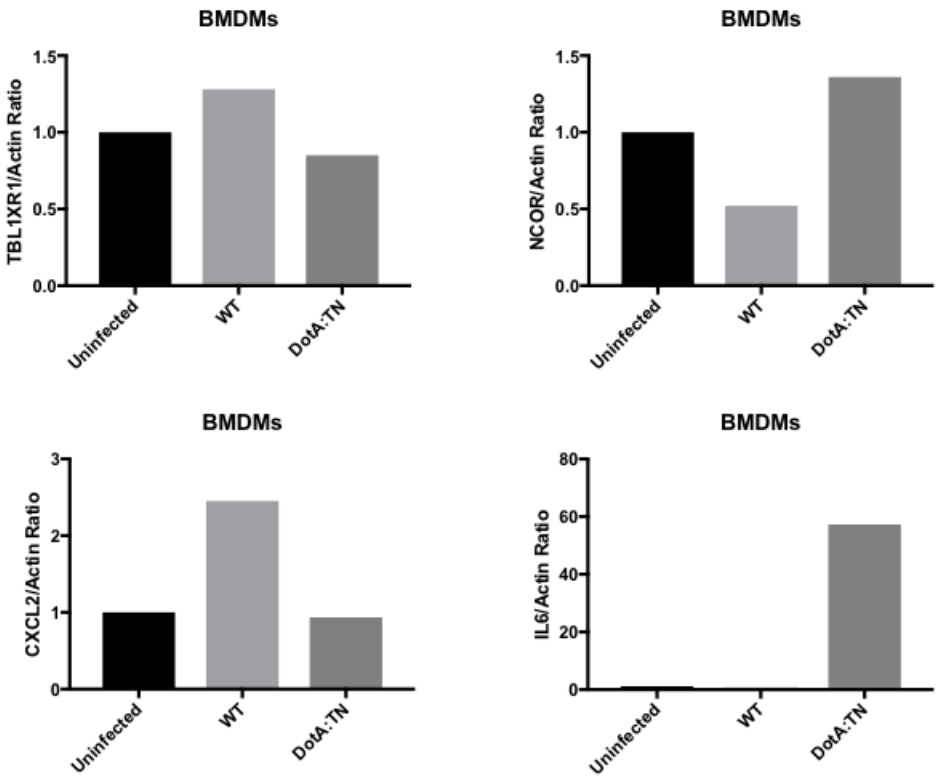

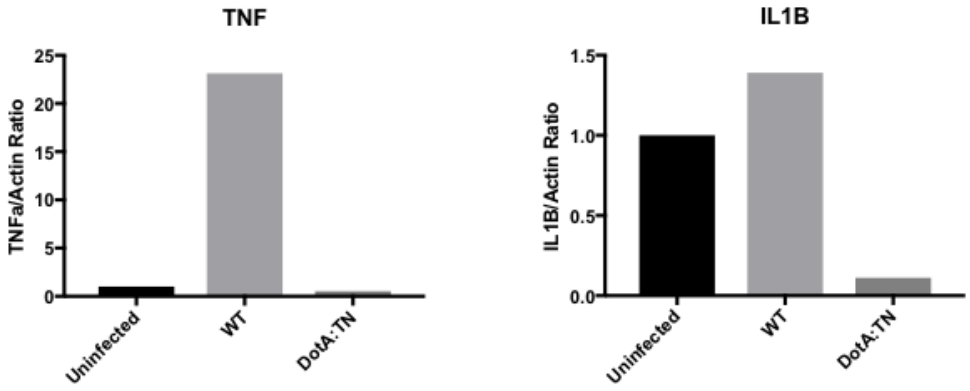

Figure A1. **Expression of TBL1XR1 related genes in bone marrow-derived macrophages.** RNA was isolated from infected BMDMs 24 hours after infection. qRT-PCR was done for specific immune genes as shown. The graphs presented are one representative experiment, therefore no statistical analysis was done.

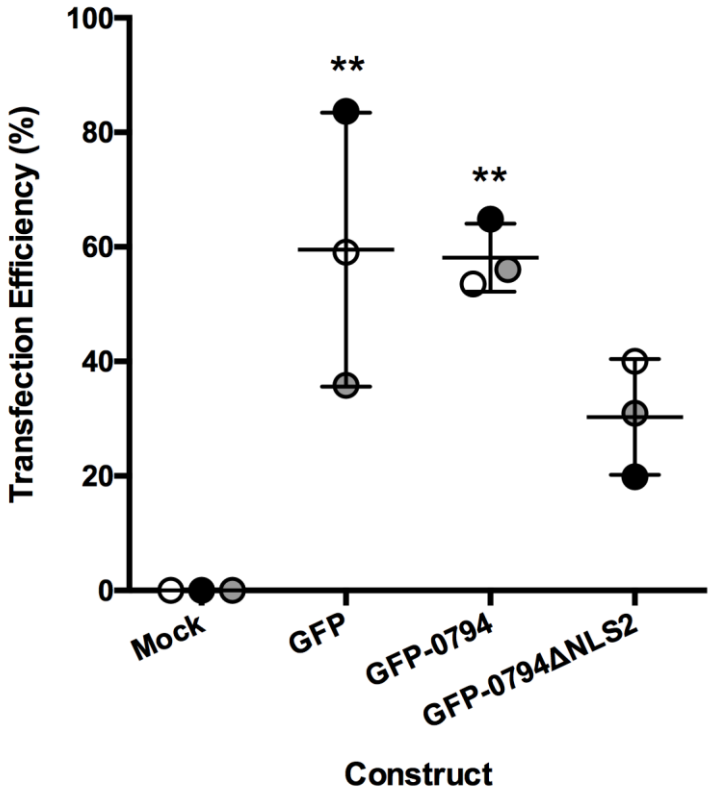

Figure A2. Transfection efficiency of constructs for RNA-seq. In order to be assured of both adequate and similar transfection rates for comparison during the RNA-seq, we compared transfection efficiency from all three replicates. The CBU0794 construct had more consistent transfection rates, but it was significantly higher than the CBU0794ΔNLS mutant.

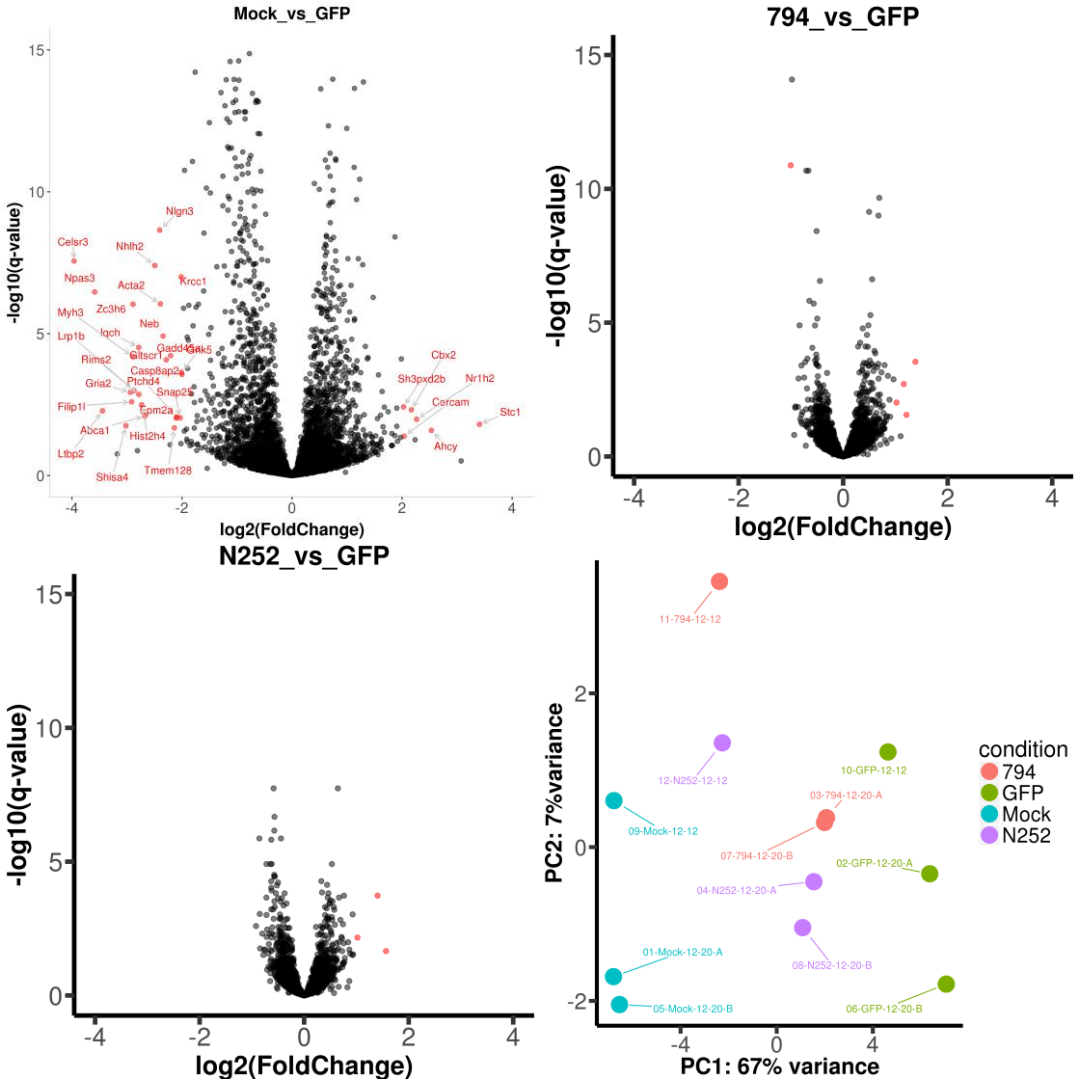

Figure A3. Additional RNA-seq analysis figures. The first three panels are volcano plots showing each individually expressed transcript. The last panel is a principal component analysis (PCA) of each replicate.

Elav4
Ska2
Macrod1
Dlk2
Mrps18c
Spata18
Nfasc
Esd
Ubxn2b
Naf1
D630045J12Rik
Mir196b
Ttc39a
Nap1l2
Hey2

Figure A4. Up-regulated genes specific to CBU0794 expression.

Sybu
Stc1
Ahcy
Nr1h2

Figure A5. Down-regulated genes specific to CBU0794 expression.

APPENDIX B

To ensure the growth defect seen in the CBU0388::tn mutant was not a result of fitness of the mutant itself, we tested a growth curve in ACCM-2 axenic media.

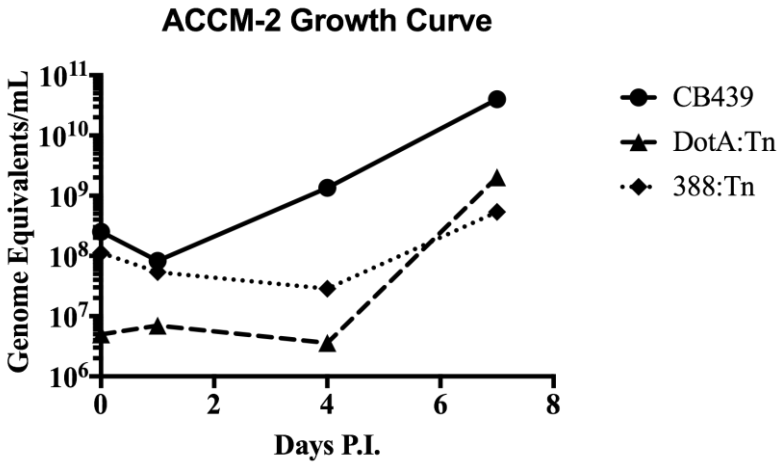

Figure B.1 Growth defect of CBU0388::tn transposon mutant is not due to fitness of bacterial strain. qRT-PCR was done on each strain grown in ACCM-2 for up to 7 days. Samples were collected at day 1, day 4 and day 7.

APPENDIX C

One of the hypotheses that developed from CBU0388's structural homology to Crm1 was potential disregulation of the molecule RAN, which acts as the key energy source for nuclear import and export. We tried several ways to test this, but ultimately concluded that while it does appear that RAN is somehow manipulated during infection, it is probably not a direct result of CBU0388 action.

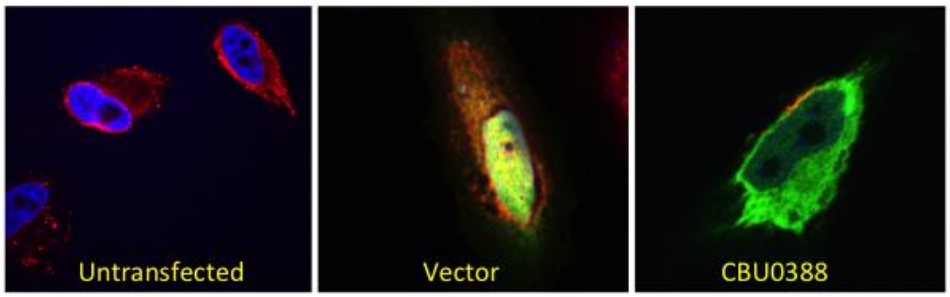

Figure C.1 RAN Expression during transient transfection of CBU0388. HeLa cells were transfected with either pEGFP-C1 vector of pEGFP-C1 CBU0388. Twelve hours post-transfections, cells were fixed and stained for RAN. Merged images are shown above. The amount of RAN present in cells transfected with CBU0388 appears to be much lower, but this may be an artifact of high cellular toxicity in these cells. Cell nuclei are stain blue with Hoescht. RAN is stained with red. GFP is stained green.

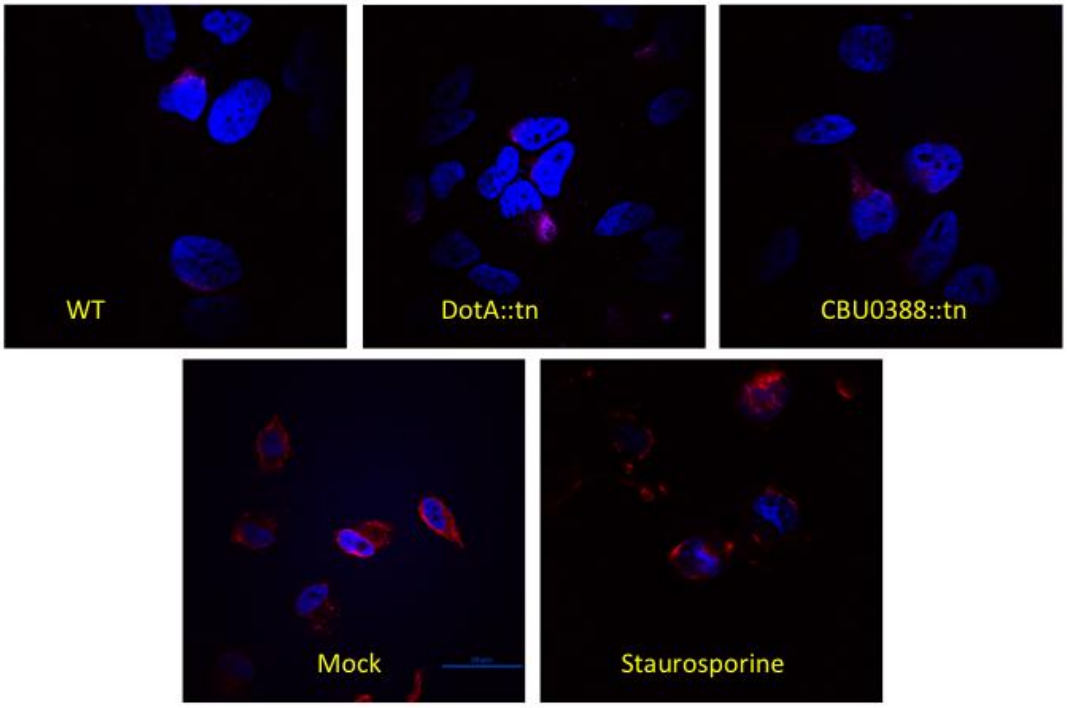

Figure C.2 RAN Expression in Infected HeLa cells. HeLa cells were infected with each indicated strain normally and fixed at four days post infection. Staurosporine treatment is used as an additional comparision. Merged images are shown above. Cell nuclei are stain blue with Hoescht. RAN is stained with red. LAMP1 is used as a marker of bacterial vacuoles stained far red.

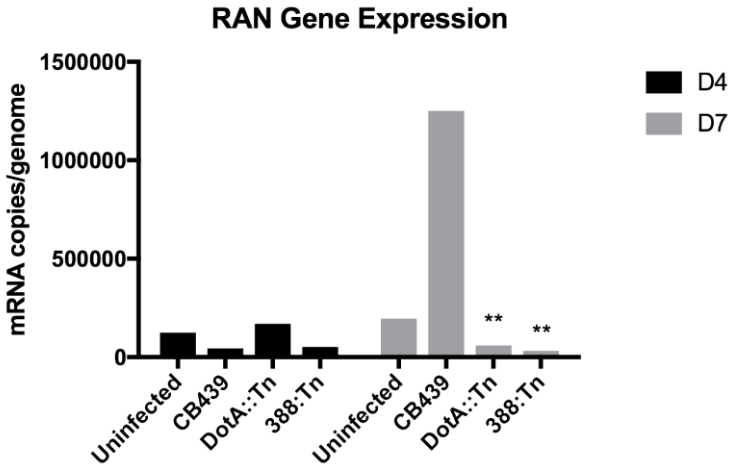

Figure C.3 Gene Expression of RAN during infection. HeLa cells were infected normally and RNA isolated at both four or seven days post-infection. Quantitative PCR was done to test for levels of RAN in each sample. Data is from a single experiment with three technical replicates. Statistics compared DotA::Tn and 388::Tn to CBU439.

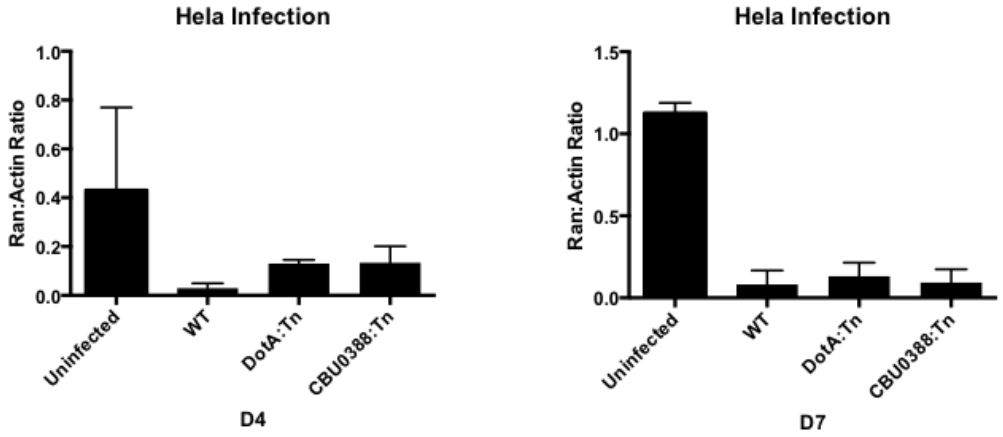

Figure C.4 RAN protein levels are modulated during infection independently from Type IV Secretion. Western blot of infected HeLa cells were done at either four or seven days post-infection. Samples were blotted for RAN and Actin as a loading control. Graph is quantitative ratio from three separate experiments. While the proteins levels of RAN appear to be significantly lower in infected cells than uninfected, this does not appear to be dependent on a functional T4BSS. Statistical analysis was not done.

(A)

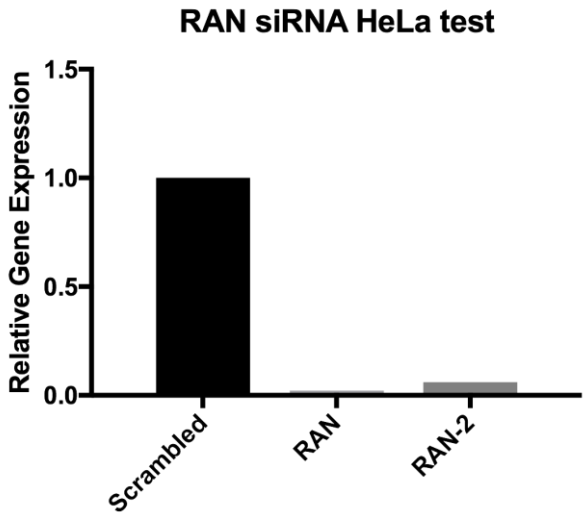

(B)

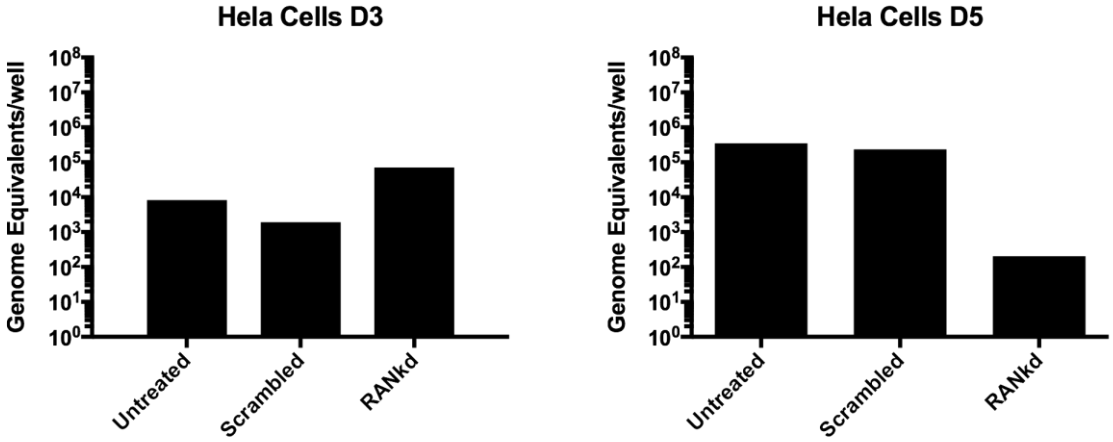

Figure C.5 Knockdown of RAN during infection in HeLa cells. (A) Transient knockdown of RAN successfully diminished the expression of RAN in HeLa cells compared to the scrambled DNA control. (B) HeLa cells were infected with wild-type *C. burnetti.* At twenty-four hours post-infection, cells were treated with the siRNA to knockdown the expression of RAN. At days 3 and 5 post-infection, cells were analyzed for replication. At day 5-post infection, there appeared to be a marked decrease in the

replication of *C. burnetii* compared to the controls. Graph shows the means from one representative experiment.

APPENDIX D

The current and most effective strategy for complementation of the CBU0388::tn mutant so far has been the use of an inducible plasmid, shown in Figure C.1. This plasmid contains an anhydrotetracycline-inducible promoter, 4xHA tag, a Kanamycin and Ampicillin resistance casette, and a Tn7 transposon. CBU0388 was able to be successfully cloned into this plasmid and transformed into *C. burnetii* successfully along with the helper Tn2 plasmid, which contains the transposase. PCR of multiple *C. burnetii* clones have shown the insertion of the Kanamycin resistance cassette in the genome, as seen in Figure C.2. Induction of the 4xHA-tagged CBU0388 appears to be somewhat successful. As seen in Figure C.3 when probed for the HA tag, you can detect tagged CBU0388. Unfortunately, the product appears to be C-terminally cleaved as you see multiple smaller fragments with the HA tag which is on the N-terminus of the protein.

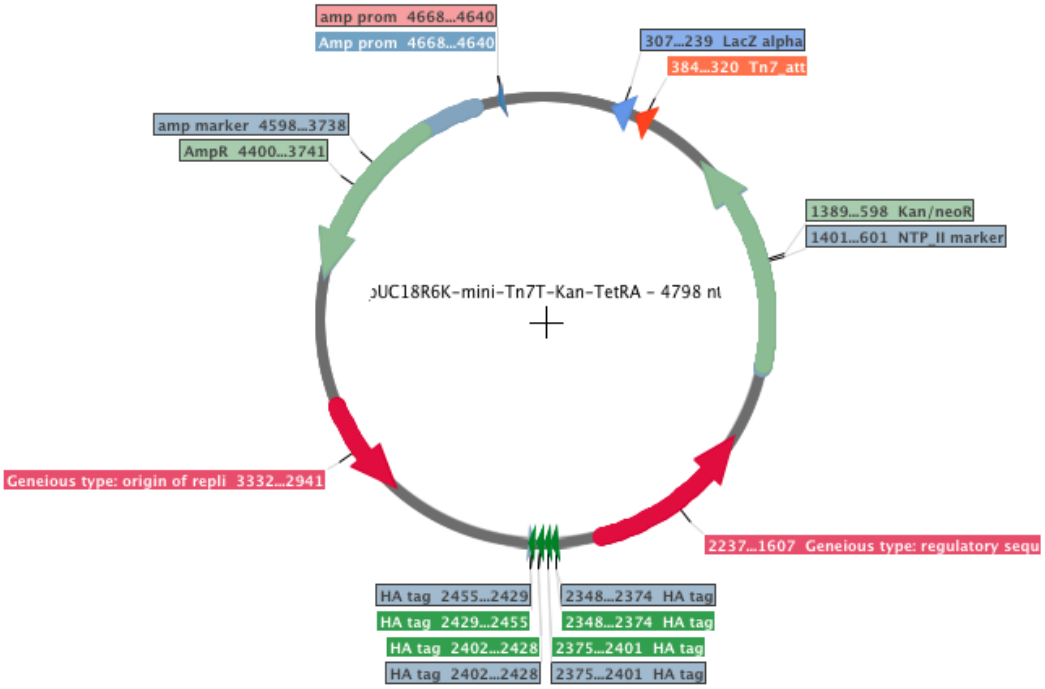

Figure D.1. Plasmid delivery vector for Tn7 Tet^{R}-Inducible 3xHA-tagged CBU0388. Plasmid map made with Serial Cloner showing antibiotic selection, marker, and Tn7 promoter. Plasmid is used in combination with commercial Tn2 helper plasmid.

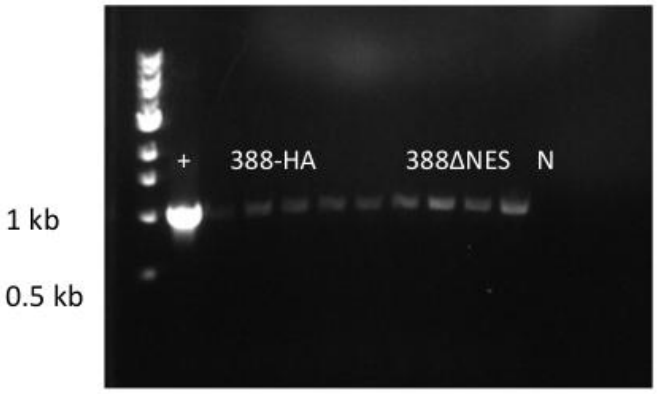

Figure D.2 PCR check for Kanamycin in multiple *C. burnetii* clones. Multiple *C. burnetii* clones transformed with CBU0388-HA plasmid or CBU0388ΔNES-HA plasmid were checked for Kanamycin insert in genomic DNA. Positive control is Kanamycin in original vector. N is negative control.

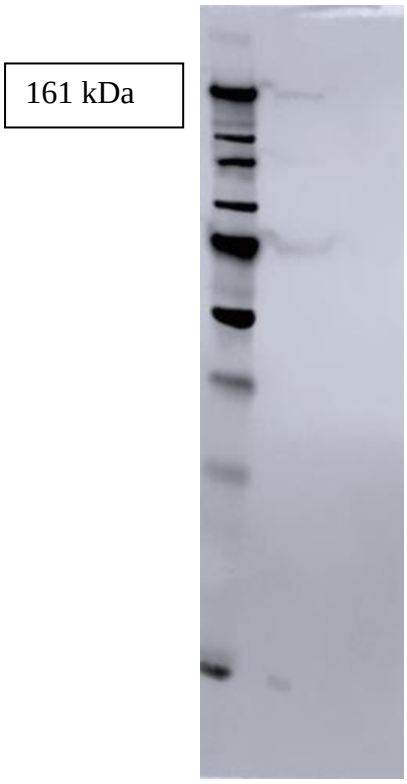

Figure D.3. Induction of CBU0388 in ACCM-2 grown bacteria. Western blot of induced expression of 3xHA-tagged CBU0388 in the CBU0388::tn mutant. Multiple bands present was typical of all experiments most likely due to degradation by C-terminal cleavage of the protein from over-expression, resulting in smaller bands.

APPENDIX E

Protein pulldown of CBU0388 ΔNLS and CBU0388 ΔNES compared to pEGFP-C1 vector in 293T cells failed to produce a reasonable list of unique protein interactions. This could be due to CBU0388 interacting with a plethora of proteins in a non-specific way. Most likely, though, we did not achieve a good expression level of CBU0388 ΔNLS and CBU0388 ΔNES to produce a specific result.

Deletion E & L
GRP75; Glucose related protein 75
RSSA 40S ribosomal protein
PHB2 Prohibitin
SERA; D-3-phosphoglycerate dehydrogenase aka PHGDH
LDHB; lactate dehydrogenase B chain
RU2A; U2 small nuclear ribonucleoprotein A
RA1L2; nuclear ribonuceloprotein A1
PCBP2; Poly (r:C) binding protein 2
TCPQ; T-complex protein 1 subunit theta
KPYM; pyruvate kinase
ALDOA; Fructose-bisphosphate aldolase

LDHA; lactate dehydrogenase chain A
CAZA1/ F-actin capping protein subunit alpha

Figure E.1. Protein results seen in both the CBU0388 ΔNES and CBU0388 ΔNLS mutants from pulldown.

Deletion E only
Parp1
FUB2; far upstream binding element
RL40; 60S ubiquitin ribosomal L40
TCPB; T-complex protein 1 subunit
CALX; Calnexin
C1QBP; complement component 1 Q subcompotent binding protein

Figure E.2. Unique protein results seen in only the CBU0388 ΔNES mutant from pulldown.

APPENDIX F

A previous paper [84] concluded that CBU0388 played a role in preventing activation of the Cell wall integrity (CWI) MAPK pathway. This paper used yeast to screen a number of *C. burnetii* effector proteins. CBU0388 is not just toxic when expressed in mammalian cells, but also yeast. This paper utilized this fact and used specific deletion mutants in the CWI pathway to compare the toxicity of CBU0388. They found that deletion in *bck1* and *mpk1*, equivalent to map3k and mapk respectively, resulted in alleviating the toxicity caused by CBU0388. With this implication that CBU0388 prevents MAPK pathway activation, we tried to confirm this in mammalian cells. The difficulty was that the CWI pathway is highly conserved in fungal cells, but doesn't have a direct equivalent in mammalian cells. We therefore tested multiple MAPK pathway inhibitors in their ability of alleviate toxicity of transfected CBU0388 in HeLa cells. We used four different inhibitors: U0126 (ERK1/2 inhibitor), SB203580 (p38 inhibitor), SP600125 (JNK inhibitor), and Dexamethasone (pan-MAPK inhibitor). Results shown in Figure F.1 show that we could not find any inhibitor that prevented the cellular toxicity caused by CBU0388. We therefore, could not tie CBU0388 to the mammalian MAPK pathway. Of course, the MAPK pathway is extremely involved with a number of other molecules playing a role in signaling. Therefore, this experiment does not completely rule out the involvement of CBU0388 in modulating some form of the mammalian MAPK pathway.

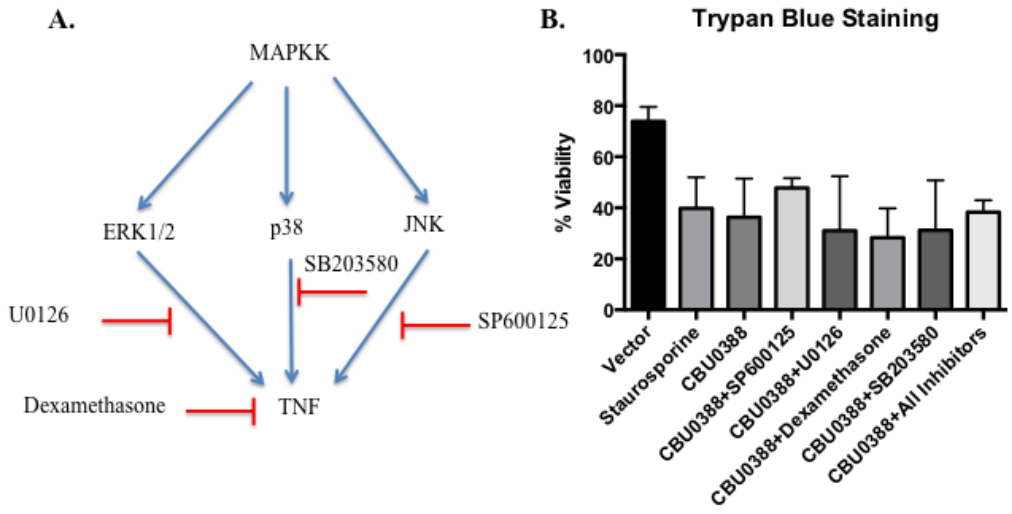

Figure F.1. MAPK inhibitors don't rescue cellular toxicity seen by CBU0388 in HeLa cells. (A) Schematic depicting the MAPK branches and targets of each pharmacological inhibitor used in this experiment. (B) Trypan blue staining to assess cellular toxicity of cells transfected with CBU0388 with or without pharmacological inhibitors. Staurosporine is used as a positive control for inducing toxicity. Graph shows the average +/- SD of three independent experiments. Statistical analysis revealed results were non-significant compared to CBU0388 transfection alone.